NTNU
Innovation and Creativity

Gas cleaning with Granular Filters

Ingunn Roald Natvig

Master of Science in Energy and Environment
Submission date: July 2007
Supervisor: Otto Kristian Sønju, EPT

Norwegian University of Science and Technology
Department of Energy and Process Engineering

Problem Description

Bakgrunn og formål

I den senere tid har en i Norge fått stadig strengere krav til rensing av røykgasser fra forskjellige typer forbrenningsanlegg og industrielle prosesser. For tiden pågar det flere prosjekter ved NTNU der gassrensing med granulært filter er et viktig element.
BioSOFC-prosjektet tar for seg kraft- og varmeproduksjon med brenselceller fra et biomassegassifiseringsanlegg i Østeriket. Hadelandprosjektet ser på rensing av avgasser fra flisforbrenningen på Bjertnes Sag A/S. I begge prosjektene brukes granulære filtre for gassrensingen.

På verdensbasis er det i tillegg til granulære filtre, mest fokus på keramiske og metalliske filtre. Ved institutt for energi- og prosessteknikk utvikles det en ny type louvergeometri for neste genrasjons "Panel bed filter" (PBF). Granulære filtre tåler høye temperaturer og kombinert med mulighetene for kjemisk prosessering av gassen er PBF teknologien et lovende alternativ for slike anvendelser. Denne rensemetoden benytter granulær filtrering og opereres med overflaterensing.

Mål

1. Kandidaten skal beskrive i detalj et renseanlegg med Panel Bed Filter for industriell gassrensing. Anlegget skal dimensjoneres ut fra gitt informasjon.

2. Det skal bygges en testenhet for en ny louvergeometri design. Kandidaten skal i den forbindelse:
   a) Sette opp testenheten
   b) Utføre utvalgte tester på enheten
   c) Optimalisere geometrien til testenheten med tanke på trykkpulsrensing av filteret for Olivin AFS30 og Sintered Bauxitte 20/40.

3. Kandidaten skal utføre utvalgte tester på en Panel Bed Filter enhet hvor resultatene skal bearbeides og presenteres.

4 Kandidaten skal utarbeide forslag til videre arbeid inkludert videre forsøk samt eventuelle forbedringer av renseanlegget.

Assignment given: 05. February 2007
Supervisor: Otto Kristian Sønju, EPT

Abstract

The panel bed filter (PBF) is a granular filter patented by A. M. Squires in the late sixties. PBFs consist of louvers with stationary, granular beds. Dust is deposited in the top layers and on the bed surface when gas flows through. PBFs are resistant to high temperatures, variations in the gas flow and hot particles. The filter is cleaned by releasing a pressure pulse in the opposite direction of the bulk flow (a puff back pulse). A new louver geometry patented by A. M. Squires is the filter tray louvers. The new design is believed to reduce the pressure drop and the number of louvers, and to make the filter more compact.

We have designed and built a laboratory scale PBF with filter tray louvers based on the patent. Experiments with the prototype show that the new louver can be cleaned with a puff back pulse.

A PBF system for a hypothetical biomass combustion plant has been designed. The heat from the flue gas will be used for district heating. The proposed PBF system design consist of double-sided modules with 46 filter tray louvers on top of each other. Five modules are mounted together in module columns, sharing the same clean gas duct and puff back pipe. The granular medium chosen is Sintered Bauxite 20/40 (SB). The module columns are placed in an enveloping house. SB and dust fall into bins in the bottom of the enveloping house during puff back cleaning. A vacuum pneumatic conveying system brings the dust and SB to the top of the filter. Dust and SB are separated in a sieve. Dust is deposited, and SB is transported back to the modules.

NTNU is currently involved in the BioSOFC project. The objective of this project is to increase efficiency in energy production from biomass by using producer gas from a biomass gasification plant in a Solid Oxide Fuel Cell. Field tests will be performed at a plant in Güssing, Austria. A PBF will be used for gas filtration. The operating temperature will be 500 °C to avoid tar condensation. We have performed heating experiments on the BioSOFC filter system. The results were not satisfactory, as the temperature in the filter ranged from 384 to 625 °C. The filter system was due to be shipped, and new tests could not be performed. This work proposes that modifications to the heating cable circuits are made, and new heating tests are performed before the field testing.

Abstract

Preface

The work presented in this thesis has been performed at the Norwegian University of Science and Technology at the faculty of Engineering, Science and Technology, at the department of Energy and Process Engineering.

The thesis covers the topics of granular bed filtration, from the theory, to the design and building process of a laboratory scale panel bed filter, to the design of a filter system for a biomass combustion plant, and to performing heating experiments on an existing filter.

I would like to thank my supervisors Daniel Stanghelle and Otto Sønju for support and guidance through my Master.

I have spent many hours in the laboratory, and I would like to thank Jan Erik Molde and the other laboratory staff for making the learning process easier.

Trondheim 19/12-2006

Ingunn Roald Natvig
Student, NTNU

Table of Contents

Contents

Nomenclature

$\overline{W_A}$	Accumulated dust load [kg/m^2]
a	Amplitude [m]
f	Frequency [Hz]
g	Gravitational accelleration [m/s^2]
P	Power [W]
R_Ω	Ohmic resistance [Ω]
t	Time [h]
V	Voltage [V]
V''	Volume flux (volume flow over filtration area) [cm/s]
A	Input value for PID controller [%]
A_b	Balanced value for PID controller [%]
$A_{filtration}$	Real filtration surface area [m^2]
$A_{nominal}$	Nominal surface face area [m^2]
c	Concentration [kg/m^3]
D	Diameter [m]
d_c	Critical separation diameter [m]
d_p	Mean particle diameter [m]
d_{50}	Median particle diameter [m]
DP	Pressure drop [bar]

g	gravitational acceleration [m/s^2]
K_1	Spesific resistence of filter medium, including deposited particles [1/s]
K_2	Spesific cake resistence [1/s]
L_gf	Thickness of filter [m]
$p_{activation}$	Activation pressure [bar]
U_s	Mean gas velocity across filter surface (Nominal face velocity) [m/s]
α_e	Constant
β	Angle of repose [°]
β_d	Angle of divergence [°]
β_e	Constant
Δ	Delta
Γ_r	Vibration intensity
κ	Porosity [m^2]
μ	Gas viscosity [kg/ms]
μ_e	Dust load in gas entering filter [kg/m^3]
μ_G	Dust load in gas exiting filter [kg/m^3]
ω	Slide angle [°]
ρ	Density [kg/m^3]
Θ	The area ratio [m^2/m^2]
Θ_e	Separation efficiency when exeeding the maximum loading of a cyclone [-]
Θ_i	Separation efficiency in vortex flow of a cyclone [-]
Θ_{total}	Total separation efficiency [-]
ΔP	Differential pressure [bar]
c	cycle

Cake	Dust cake
Filter	Filter
Olivine	Olivin AFS30
PBF	Panel bed filter
PID	proportional-integral-derivative (PID-controller)
SB	Sintered Bauxite 20/40
SOFC	Solide oxide fuel cell

List of Figures

List of Tables

List of tables

Chapter 1

Introduction

1.1 Background

Increased energy production, and increased focus on the environmental consequences, has led to a rise in the demand for efficient cleaning technologies. Today, only moderate temperature gas treatment technologies such as fabric filters are commercially available. High temperature gas cleaning significantly increases energy efficiency. The panel bed filter (PBF) is a promising gas cleaning technology due to its rigidity. The PBF is resistant to high temperatures, variations in gas flow, and to hot particles and other contaminants that may be present in high temperature gas. The granular filter was patented by A.M. Squires in the late sixties [1], and has been under development at NTNU. The filter tray louver is a new louver geometry patented by A.M. Squires [5]. The new geometry is believed to increase space efficiency and to reduce pressure drop and costs.

Part of this thesis is associated with the BioSOFC project, an co-operative project with partners NTNU, Prototech AS and Vang Filter Technologies AS. The project objective is to obtain higher efficiency in bio-energy production using a solid oxide fuel cell (SOFC). Producer gas from a gasification plant in Güssing, Austria is to be filtrated in a PBF, before it is fed to a SOFC. Field testing is planned this summer.

1.2 Thesis objective

The purpose of this thesis has been to further develop the panel bed filter technology. The main objectives have been:

- To build, evaluate and optimize a panel bed filter with the new louver geometry

- To design an entire filter system for a hypothetical bio-combustion plant
- Experimental tests and preparations of the BioSOFC filter before it is shipped to Güssing

The first and the last objective are experimental of nature, resulting in plenty of time spent in the laboratory. The knowledge acquired through hours spent in the laboratory are hardly reflected in this thesis. The third objective was a literature study.

1.3 Thesis overview

Chapter 2 deals with the theory of granular filtration and of the panel bed filter, including filtering mechanisms, pressure build up and filter operation. The thesis has been divided into three parts solving the three objectives of the work. The three parts are found in chapter 3 through 5.

The new louver geometry is presented in chapter 3. The chapter includes a short summary of historic louver designs, and a presentation of the filter tray louver. The design of a laboratory scale PBF with filter tray louvers, and the experimental work done with the prototype are also found in the chapter. The time available for experimental tests has been limited due to other projects requiring laboratory resources. The prototype has only been tested with Sintered Bauxite 20/40 (SB), and not with Olivine AFS30 (Olivine) as first intended.

Chapter 4 presents the design of a specific panel bed filter system. The system includes a cyclone, a PBF module design, sand recycle system and puff-back regeneration system.

Chapter 5 includes a description of the BioSOFC filter and the results from heating and puff back experiments.

Conclusions from the the three parts of the thesis are found in chapter 6. The chapter also includes recommendations for further work.

Chapter 2

The theory of panel bed filtration

A granular filter is a cleaning system utilizing a granular medium in the separation process [2]. PBFs consist of stationary granular beds. The gas flows through, and dust is deposited in the bed and on the bed surface.

2.1 Filtering mechanisms

Experiments have shown that dust particles can be separated from a gas stream when flowing through a granular bed. The mechanisms involved in the separation, are many and complex. The most important principle is that the dust particles have to leave the path of the gas flow in order to be deposited. A granular filter will only be functional if there are transport mechanisms that cause the particles to move out of the gas flow path [2]. Adhesion mechanisms cause particles to stick to the filter medium or to previously deposited particles.

Transport mechanisms Three important transport mechanisms in PBFs are inertia forces, electrostatic forces and brownian movement.

Inertia forces occur when particles fail to follow the deflected path of the gas around the granular particles. Larger dust particles will have larger moment of inertia, and are more easily deposited than smaller particles. Higher gas velocities will also cause more depositions [2].

Electrostatic forces are present when the particles in the gas are charged. Particles can attain electric charge when hitting other particles or the walls. Agglomeration of particles with opposite charges occur. The agglomerated particles are deposited due to inertia. Charged particles can also be deposited directly on walls or on the granular medium, if the charge is correct. Ions may be present in gases at high temperatures. The ions can charge dust particles. The presence of steam in the gas reduces the chance of particles attaining electrical charge.

Brownian motion is the random motion of particles in the gas, caused by collisions between the gas molecules and particles. The movements cause diffusion, and the phenomenon increases with decreasing particle size [2].

Adhesion mechanisms The most important adhesion mechanisms are Van der Wals forces, Coulomb forces, capillary forces and stickiness. Van der Wals forces are caused be electromagnetic forces between molecules in close contact and Coulomb forces are caused by electric charges that bind the dust particles to the granular particles. The capillary forces are caused by liquid between the dust particles and the granular particles. The surface tension of the liquid, keep the particles together. Stickiness occur when partially combusted particles or condensed components such as tar are present [8].

2.2 The filter cake build up

Filter cake build up is divided into three stages; deep bed filtration, rooting cake filtration and surface cake filtration.

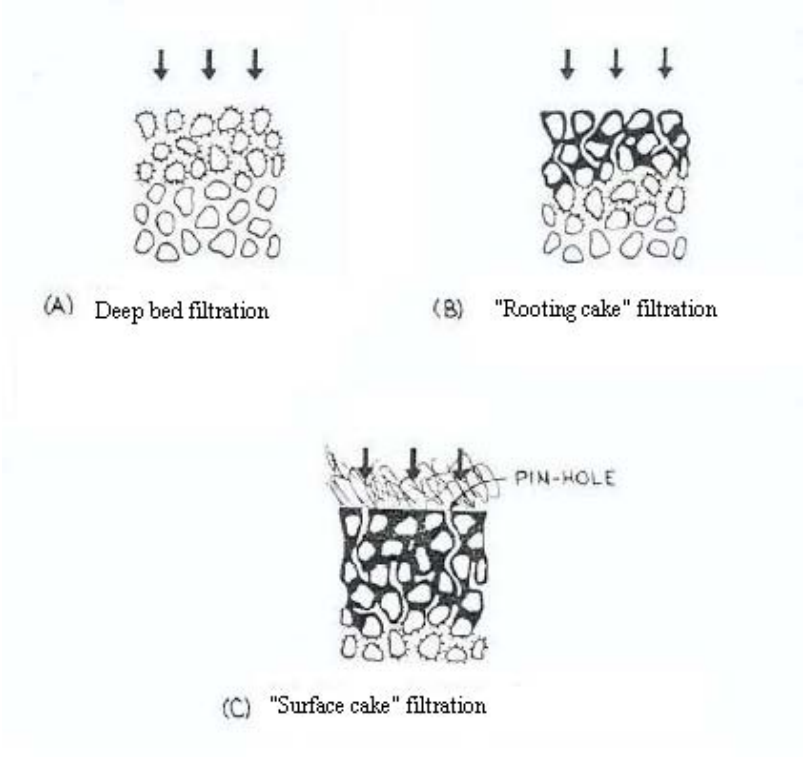

Figure 2.1: Dust cake build up [1]

Deep bed filtration During filtration through a clean granular bed, some dust particles will penetrate the top layers of the granular medium and are deposited in the bed, as illustrated in Figure 2.1 A. A lot of particles will follow the gas path through the bed, and cause filtering efficiency to be low [2].

Rooting cake filtration As dust particles are accumulated in the granular medium, they will clog the filter. This is called agglomeration. The dust lumps will make up roots in the granular medium as illustrated in Figure 2.1 B. The clogging of the filter contribute to filtrate even more dust particles due to mechanisms described in section 2.1. The separation efficiency is enhanced.

Surface cake filtration The last stage of the filter cake build up occur when enough dust particles have been deposited in the top layers of the granular medium, and cause further depositions to occur on the surface. The surface depositions make up an even filter cake as illustrated in Figure 2.1 C. The separation efficiency is further enhanced due to a reduction in the void fraction (the volume not occupied by particles) when dust is deposited. The reduction of paths through the filter, cause an increase in the pressure drop.

2.3 Puff back cleaning

The core of the PBF technology is the puff back cleaning: Filter cake is removed by releasing a pressure pulse (puff back pulse) in the opposite direction of the bulk flow. The sandspill is the granular medium removed during puff back cleaning. Only the top layers of the granular medium should be removed, leaving the dust roots. Using SB as filtration medium, ideal sandspill is calculated (using the bulk density) to be between 1,3 and 2,7 kg/m^2. The ideal sandspill depends on how the medium is packed.

2.3.1 The PBF cycle

A PBF operation cycle (puff back cycle) is illustrated in Figure 2.2. Gas is filtrated when flowing through the PBF (Figure 2.2 A). Puff back cleaning is initiated when a certain amount of dust is accumulated on the filter surface (Figure 2.2 B and C). Fresh granular medium is supplied (Figure 2.2 D), and the cycle starts over.

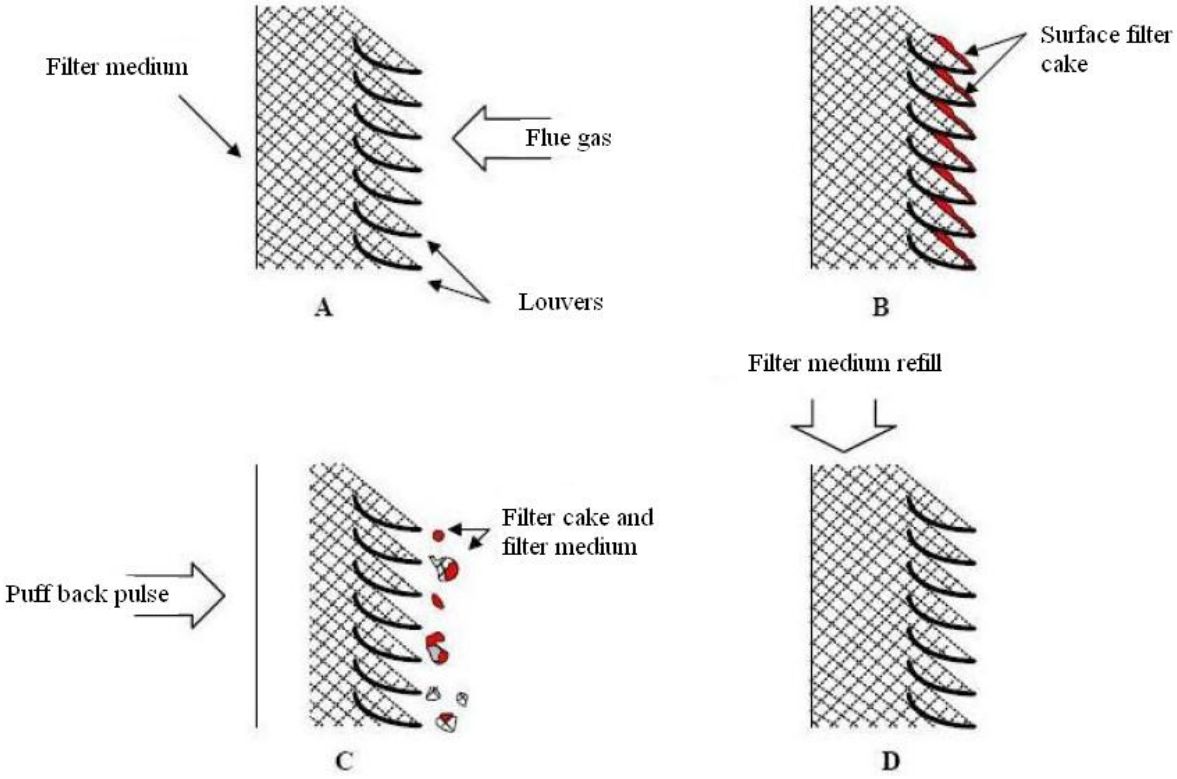

Figure 2.2: PBF cleaning cycle [2]

2.3.2 Activation time and activation pressure

Experiments performed by Lee [1] led to the active time theory: The amount of sandspill during puff back depends on the amount of time the pressure drop over the granular bed exceed a minimum pressure drop, $\Delta P_{activation}$. Figure 2.3 illustrates an ideal, triangular pressure pulse. According to the active time theory, the maximum pressure has no consequence on the amount of sandspill. Lee performed

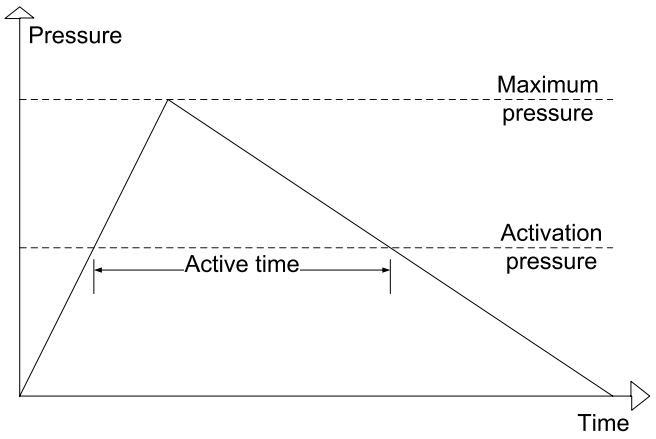

Figure 2.3: Activation time [1]

experiments with 10-40 mesh sand, and found the activation pressure to be 8,3 mbar for puff back pulses released vertically from above [1]. The activation pressure for horizontal puff back pulses was 5,3 mbar. Risnes [4] performed similar experiments on a PBF with vertical puff back, and found activation pressure to range from 5 to 9 mbar . Risnes did not support Lee's active time theory, but found (through experiments) a correlation between the sandspill and the amount of air with a pressure above $\Delta p_{activation}$ passing through the granular bed given by equation 2.1.

$$\int_{t1}^{t2} (\Delta P - \Delta P_{activation}) dt \tag{2.1}$$

$t1$ is the time at the beginning, and $t2$ is the time at the end of the pressure pulse. The difference in the two theories may have been caused by the valves used in the experiments. Lee used a rapid cylinder valve with an opening time of 15 to 20 ms. Risnes used a FESTO CPE14 valve with an opening time of 25 ms. Therefore the pressure pulse in Lee's experiments could have been more intense than for the Risnes experiments [8].

2.3.3 The stages of sandspill

Lee performed puff back experiments on a PBF recording the sandspill from the louvers with a high speed camera [1]. The movies revealed that the sandspill could be divided into three stages shown in Figure 2.4. During the first stage, the sand jumps from the inner edge of each sand surface as illustrated in Figure 2.4 (a). Only few milliseconds later, the bulk of the sand moves forward. The spurting from the inner edges of the sand surfaces stops. The bulk movement is the second stage illustrated in Figure 2.4 (b). The stage lasts from 10 to 100 milliseconds depending on the intensity of the puff back pulse. Most of the sandspill falls off the louver surfaces during this stage. The third stage, illustrated in Figure 2.4 (c), lasts several times longer than the second stage, and can be described as an after-spill. Only a few sand grains fall from the outer edges of the sand surfaces [1].

The three stages can be explained with soil mechanics [1]. The first stage results from local failure at the inner edges of the sand surfaces. The second stage, or the bulk movement stage, results from body failure. Lee believes that the second stage occur when aerodynamic forces acting on the sand bed are larger than the strength of the bed [1]. During the second stage, the sand is blown into a structure that is not stable according to the angle of repose (the maximum angle of a stable slope specific to each granular material). During the third stage, some sand is removed during stabilization of the bed [1].

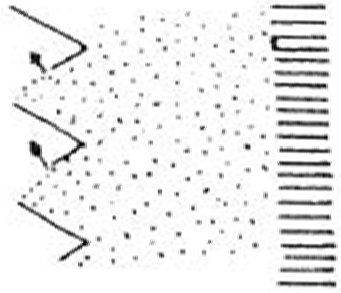

(a) First stage:
local failure near
inner edge of each
gas-entry surface.

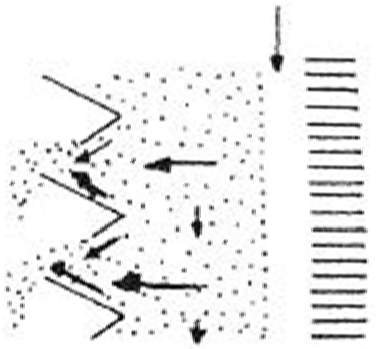

(b) Second stage:
body failure and
separation.

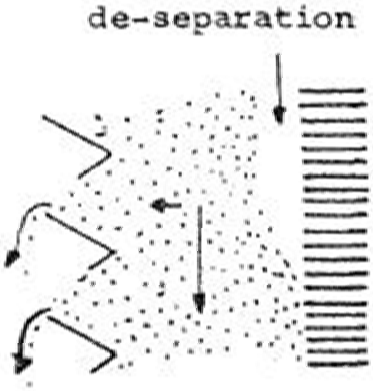

(c) Third stage:
gravity motion downward,
de-separation, and
afterspill.

Figure 2.4: Three stages of sand motion during puff back [1]

2.4 The PBF pressure build up

2.4.1 Darcys law

Darcy's law describe one-directional laminar flow through a porous medium filled with fluid [9]. Henry Darcy determined the relation experimentally. The law is based on the principle of conversion of momentum, and states the simple, proportional relationship between the volume flow Q through a porous medium, viscosity μ and pressure drop ΔP over a distance L [9]. Darcys law can be written as:

$$Q = \frac{-\kappa A}{\mu}(\frac{\Delta P}{L} + \rho g sin\alpha) \tag{2.2}$$

The permeability κ denotes the ability of the porous medium to transmit a fluid, and A is the flow cross section. The term $\rho g sin\alpha$ accounts for the effect of gravity. g is the gravitational acceleration, and ρ is the density. α is the angle between gravity and the direction of the flow. The pressure change is negative by convention, because the fluid will flow from a high pressure to a low pressure.

2.4.2 Porosity and basic particle characteristics

The porosity, κ, for a granular bed with almost spherical particles depends on how the particles are packed. The most compact packing is face centered cubic packing, illustrated in Figure 2.5 a. The least compact way of packing spherical particles is by placing them on top of each other as illustrated in Figure 2.5 b. ω denotes the

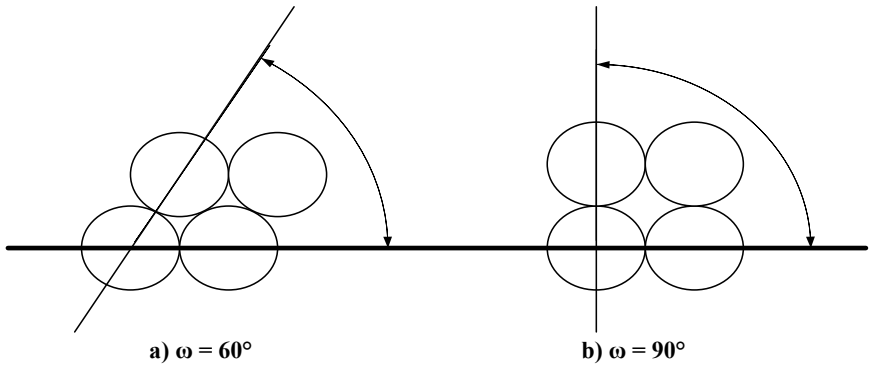

Figure 2.5: Packing of spherical particles [2]

angle between the particles, and can be used in calculations of the porosity κ [2]:

$$\kappa = 1 - \frac{\pi}{6(1 - cos\omega)\sqrt{1 + 2cos\omega}} \tag{2.3}$$

The porosity for the two extremities illustrated in Figure 2.5 is 0,260 and 0,476. This porosity is calculated for perfectly spherical particles.

The porosity depends upon the geometrical shape of the particles. Particles are often described by equivalent diameters. An equivalent diameter is defined as the diameter of a sphere which has the same feature as the irregularly shaped particle. Some useful particle diameters are [3]:

- x_{PM}: The diameter of a sphere with the same projected surface area
- x_S: The diameter of a particle with the same surface area
- x_V: The diameter of a particle with the same volume

The shape of particles can be irregular, and the geometry is not easily defined. One equivalent diameter is not enough to describe the geometric shape of a particle. Often more than one diameter is combined to characterize the geometric shape. A common ratio used to define the particle shape is the spherisity ψ, defined by Wadell [3]:

$$\psi = \frac{x_v^2}{x_s^2} \tag{2.4}$$

Shperisities between 0,45 and 0,97 is illustrated in Figure 2.6

2.4.3 Granular filter pressure drop

For most systems, measurements of dust cake during operation are not feasible. The cake properties can be calculated from the pressure drop; a parameter that is easily measured. The pressure drop ΔP over a filter is the sum of the filter material pressure drop and the dust cake pressure drop:

$$\Delta P = \Delta P_{filter} + \Delta P_{cake} \tag{2.5}$$

Equation 2.5 can be rewritten using specific resistance K_1 for the filter medium including deposited dust, and K_2 for specific cake resistance:

$$\Delta P = K_1 \mu U_s + K_2 \mu U_s \overline{W_A} \tag{2.6}$$

μ is the gas viscosity, and U_S is the mean gas velocity across the filter surface. $K1$ and $K2$ are often used to describe the pressure characteristics of a filter. $\overline{W_A}$ is the dust load, and can be written as:

$$\overline{W_A} = cU_S t_c \tag{2.7}$$

c is the concentration, and t_c is the duration of one puff back cycle.

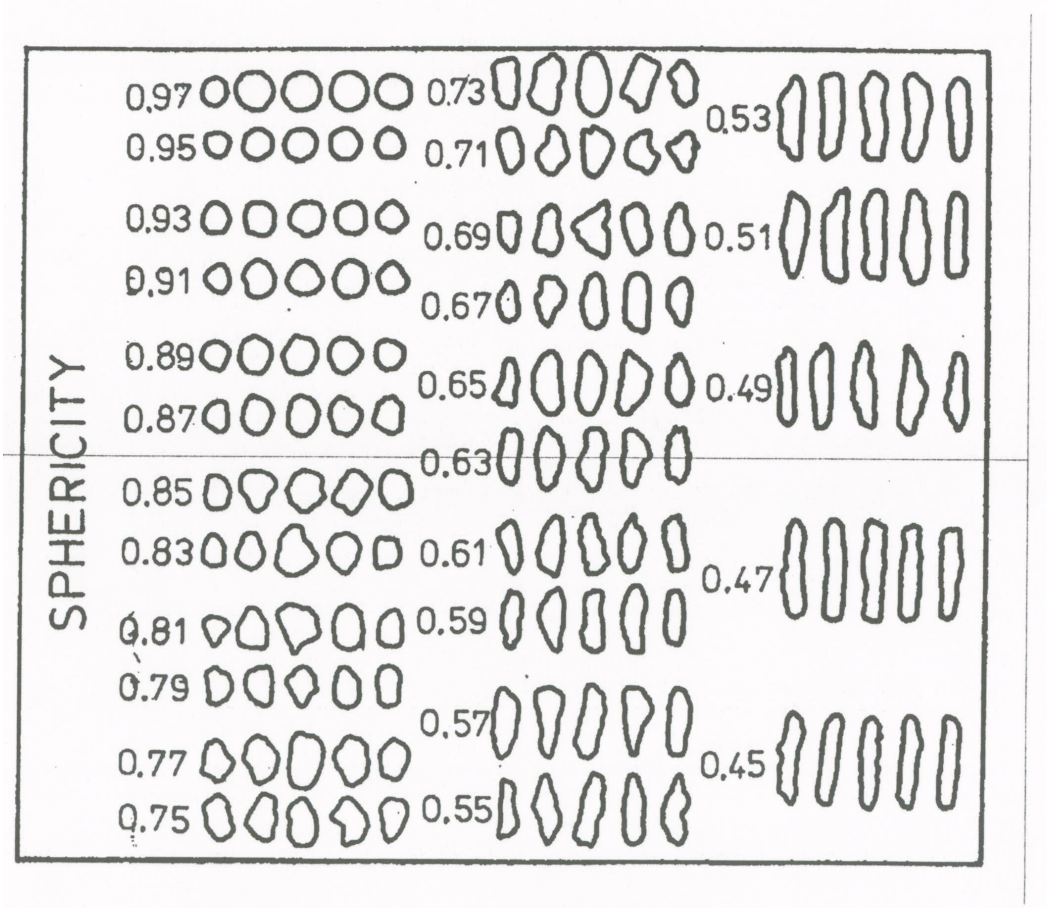

Figure 2.6: Standard table for determination of the spherisity according to Rittenhous [3]

2.4.4 Filter operation

Figure 2.7 illustrates the filter operation of a PBF. t_c is the duration of a puff back cycle, ΔP_0 is the pressure drop over a clean filter and ΔP_r is the residual pressure drop, or the pressure drop of the filter including deposited particles. ΔP_{max} is the pressure drop before puff back, and is a design criteria. The chosen value for ΔP_{max} will affect the puff back cycle and the overall system.

A low value for ΔP_{max} will lead to frequent cleaning. More pressurized air must be supplied. A high value for ΔP_{max} will lead to a greater difference in resistance between beds newly cleaned and loaded beds. The gas flow will always choose the path of least resistance, and the difference can cause high gas velocities through newly cleaned beds. A high velocity increase the chance of fluidization of the granular particles, for sand spills into the clean air duct, and for dust particles

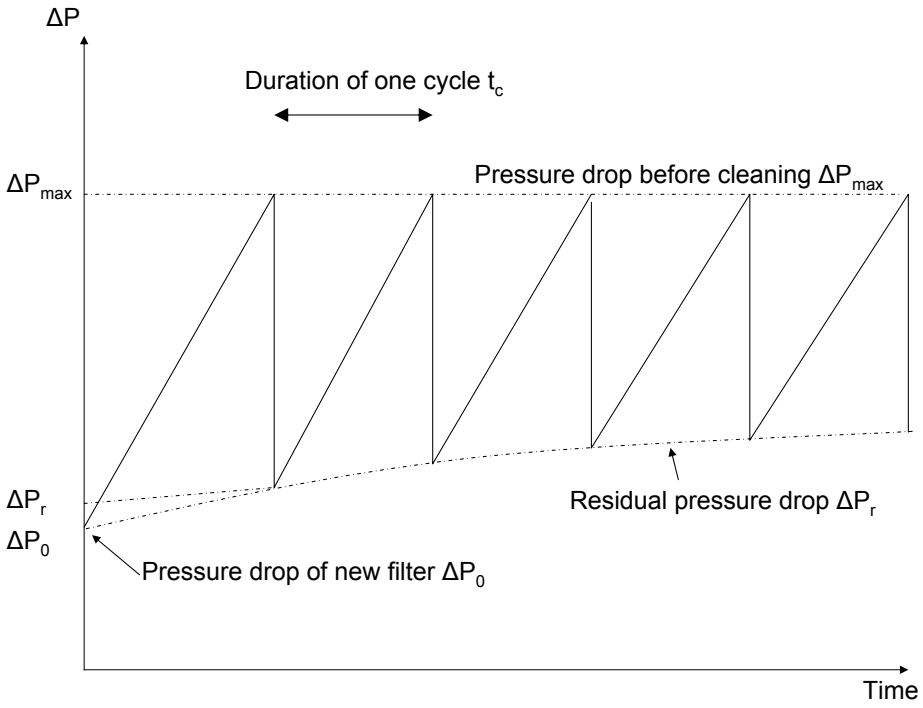

Figure 2.7: Graphical illustration of puff back cycle. Pressure drop vs. elapsed time. [4]

to penetrate the filter.

2.5 Nominal gas velocity and the area ratio

The gas flow through PBFs is normally given in terms of the nominal face gas velocity. The nominal face area $A_{nominal}$ is defined by Squires [5] as the area of a plane drawn through upper and lower edges of the louver, illustrated in Figure 2.8 A. The nominal face gas velocity U_s is defined as the average velocity through the vertical cross section of the filter front. The nominal face area differs from the area involved in filtration; the gas entry face area illustrated in Figure 2.8 A.

The area ratio Θ is the ratio between the nominal face area and the gas entry face:

$$\Theta = \frac{A_{entry}}{A_{nominal}} \tag{2.8}$$

The filtration velocity or the volume flux V'' describes the flow through the bed. V'' is defined as the average velocity through the gas entry face, and is

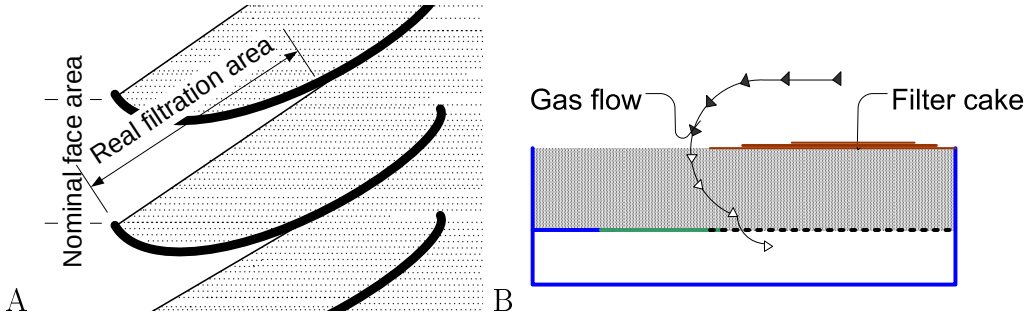

Figure 2.8: A: nominal and real filtration area B: Gas flow through dirty louver

important with respect to filter cake performance. The relation between U_s and V'' is determined by nominal face area, $A_{nominal}$ and the gas entry face, $A_{filtration}$:

$$A_{nominal} * U_s = A_{filtration} * V'' \tag{2.9}$$

Equation 2.8 and 2.9 gives the relation between the nominal face gas velocity and the volume flux:

$$V'' = \frac{U_s}{\Theta} \tag{2.10}$$

Chapter 3

New design for the panel bed filter

3.1 Introduction

Experience with the PBF technology has led to a new improved design suggested by A.M. Squires [5]. The new design strives to maximize the gas entry face, and to simplify production by reducing the number of louvers in each filter. Pressure loss will be reduced according to Darcy's law due to the granular beds being shallower. The patent [10] is the starting point of the chapter. A design of a PBF prototype with filter tray louvers for SB is a part of this work. The design variables are also found for Olivine, but the design was never made due to lack of time. The design and building process, and the experiments performed on the prototype for SB are presented in this chapter.

3.1.1 Design variables for PBFs

The first PBF was patented by A. M. Squires in the late sixties. He and his colleagues acknowledged that dust is deposited on the entry face when flue gas is filtered through a bed of a granular medium [1]. The PBF technology has been developed, and many louver designs have been suggested and tested. Designers have strived to optimize some key variables:

- By reducing the number of louvers, the production of PBF modules can by simplified. The early PBF designs were made up of many small louver plates, and the assembly was difficult. Fewer and larger louvers will lower the investment costs.

- By increasing the area ratio the footprint can be reduced. The increased gas entry surface area per nominal gas face area results in space efficiency.

- By reducing pressure drop. The money spent on fan power in large industrial plants is significant, and a low pressure drop will make the PBF technology more attractive.

3.1.2 Summary of important panel bed louver designs

An early louver design, the wishbone design, is illustrated in Figure 3.1 D. The early PBFs had many small, up sloping louvers. Later, Squires [1], recognized that louvers should slope downwards to increase the entry surface area and allowing gravity to assist the puff-back cleaning.

The louvers illustrated in Figure 3.1 and 3.2, are the most important louver designs. The down sloping design shown in Figure 3.1 A, was successfully tested by Risnes [4] at Folla in 2002. The flat plate design in Figure 3.1 B is easier to produce and assemble, but experiments showed that the design was not functional. After puff back, a narrow sand free region appeared under each louver. There has never been conducted filtration experiments with this design [5]. The design of Figure 3.2 A solved this problem. The design is simpler to produce than the Risnes design. Both have been tested in commercial scale modules [5].

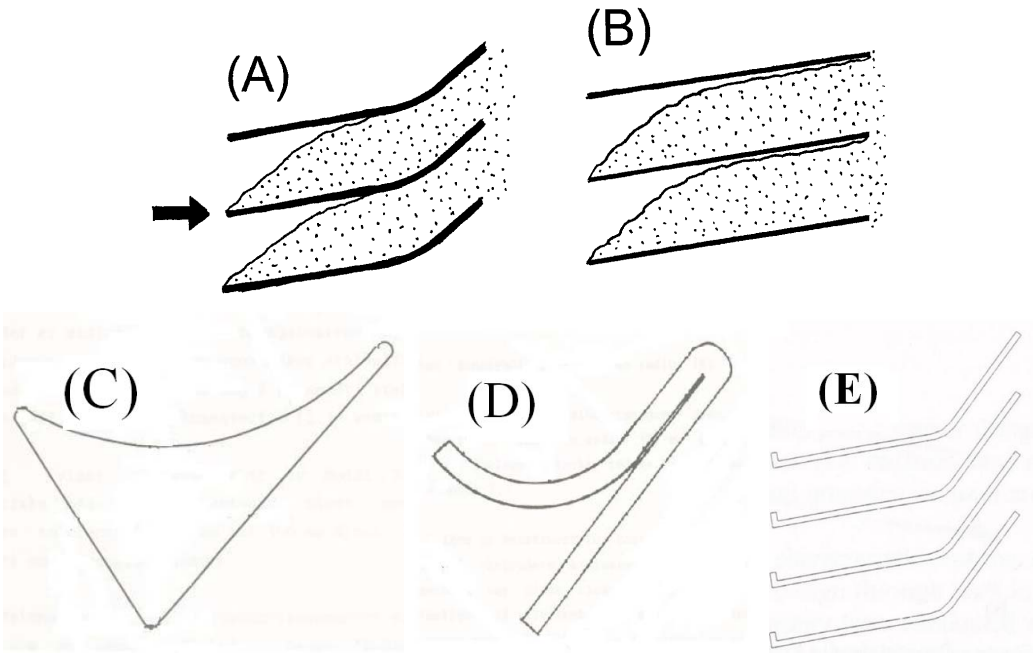

Figure 3.1: A: The R-2 louver design. B: Flat plate louver design. [5] C: The Folla louver design D: The wishbone louver design [1] E: The L10-56 louver.

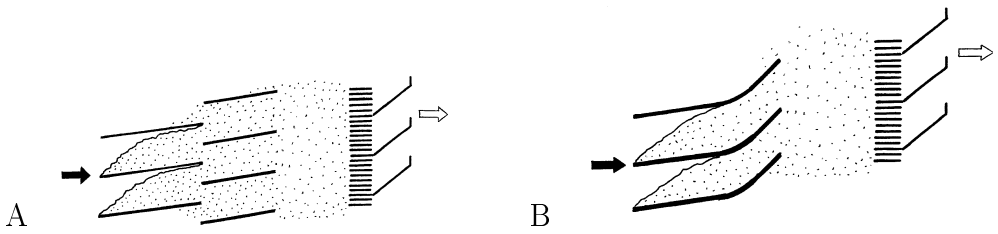

Figure 3.2: Two flat plate PBF designs tested in commercial scale [5].

The downward sloping louver design has proven to be

3.1.3 Description of the new louver design

The new design is expected to significantly reduce pressure drop and plant footprint [5]. Figure 3.3 shows three cross sections of the design. Figure 3.3 A is cross section BB of Figure 3.3 B. Figure 3.3 B is the cross section AA of Figure 3.3 A.

The filter tray consists of a permeable surface supporting a granular bed. The permeable surface can either consist of closely spaced flat plates, small-bore tubes fused together or a honey-comb structure [5]. The filter trays are sloping downward toward their outer edges. The filter trays receive granular medium from vertical pipes at the inner edge. The sand pipes are spaced together so that the permeable surface is covered with granular medium at all times, as shown in Figure 3.3 C. Figure 3.3 B shows the cross section CC of Figure 3.3 C, and illustrates the gas flow. Dirty gas (black arrow) enters from the left. Particles are filtered out on the surface of the granular bed, and clean gas flows through the permeable surface. The section under the filter tray is sealed so that the clean gas will flow past the sand supply pipes into the clean air duct (white arrow). The filter tray PBF design can be regenerated by releasing a gas pulse in the opposite direction of the bulk flow.

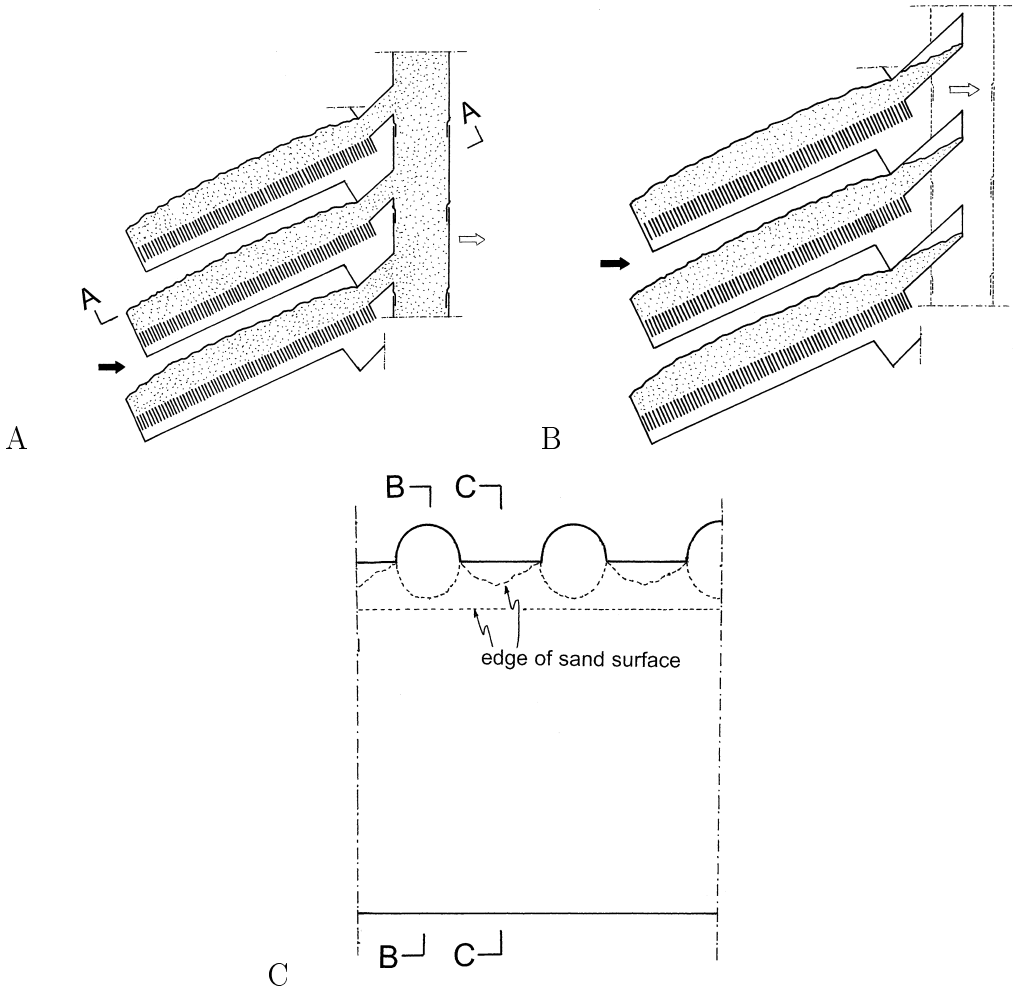

Figure 3.3: New panel bed design [5].

3.2 Design calculation

3.2.1 The angle of repose

A conic hill is formed when granular medium is poured on a flat surface. The angle between the flat surface and the surface of the hill is called the angle of repose and is a key variable when designing the filter tray louvers. To make the louver design work, the angles of the louver and the sand refill must be designed so that the penetrable surface is covered with granular medium at all times. The angle of the slanting louvers should be just below the angle of repose.

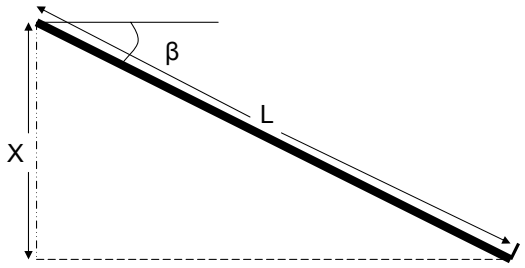

Figure 3.4: The angle of repose

We measured the angle of repose using a plastic plate with a length of L, and with a stopper at the lower end, as illustrated in Figure 3.4. The granular medium was placed on the plate and the angle was slowly increased. When the granular particles started sliding on top of each other, the height X was measured and the angle β was calculated. The angle of repose measured for the granular mediums in question is given in Table 3.1.

Granular media	L	X	angle
Sintered Bauxite 20/40	17,6 cm	6,5 cm	21,7 °
Olivin AFS30	17,6 cm	8,6 cm	29,2 °

Table 3.1: The angle of repose

3.2.2 Calculation of the sandfill openings

In Figure 3.3, there is a section of the filter tray at the upper edge, with an angle exceeding the angle of repose. This section, called the slide, is a non-permeable surface. The permeable surface has to be covered with granular medium at all times to avoid dust penetrating into the clean air duct. Therefore the angle of a line between the sand entry point and any point on the edge of the permeable surface must exceed the angle of repose. One suggested design is illustrated in Figure 3.5. The slide has the same angle as the louver. The distance from the top of the sand refill opening (hole) to the slide plate has the height AC, and the line CD has an angle exceeding the angle of repose.

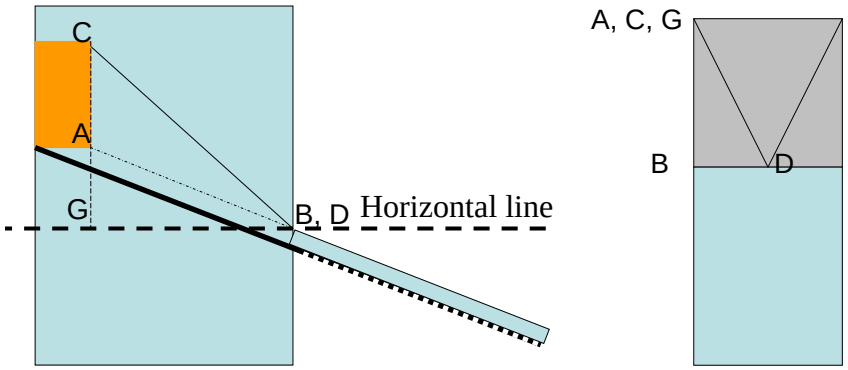

Figure 3.5: Left: Cross section of a filter tray louver design, Right: Louver from above.

The height of the sandfill opening, above the sand bed height, can be calculated using simple geometric formulas given in equations 3.1 through 3.3.

$$GB = ABcos\beta \tag{3.1}$$

$$GD = \sqrt{GB^2 + BD^2} \tag{3.2}$$

$$AC = GC - AG = GDtan\beta - ABsin\beta \tag{3.3}$$

β is the angle of repose for the granular medium. GB is half the louver width. AB is the length of the slide, and is a design parameter set to be 5 cm.

The calculations were first done evaluating the angle of a slide plate (with the length CB) corresponding to the height of the holes in equation 3.3. Angles evaluated for different slide plate lengths AB are found in Appendix B.

Using the formulas presented above, the height of the sandfill openings were calculated to be 0,6 cm for Olivin and 0,4 cm for SB (height above bed thickness).

3.3 Demonstration filter trays

3.3.1 The first demonstration louver

A filter tray test louver was built, and the sandfill arrangement was tested. One louver was mounted in the angle of repose for SB. The rectangular sandfill holes had a width of approximately 0,5 cm. The height was set to 1,4 cm, and the holes were cut out 5 cm from the grid. The sandfill boxes were filled with SB, and the louver was filled with SB flowing through the sandfill holes. The louver had a uniform bed of 1 cm, as estimated and the SB refill was successfull.

The sandfill boxes and the louver were emptied, and the louver was remounted in the angle of repose for Olivin. The height of the sandfill holes were increased to 1,6 cm. The sandfill boxes were filled with Olivin, but the holes were not large enough to fill the louver with a uniform bed. The calculations in the previous section did not take wall thickness into account. The effect of the error was larger for Olivin than for SB, due to the higher angle of repose. The height of the sandfill holes was increased to 1,75 cm, and the sandfill boxes were refilled with Olivin. The Olivin filled the louver with an even bed of 1 cm, and the sand refill was successfull.

Both beds are illustrated in Figure 3.6.

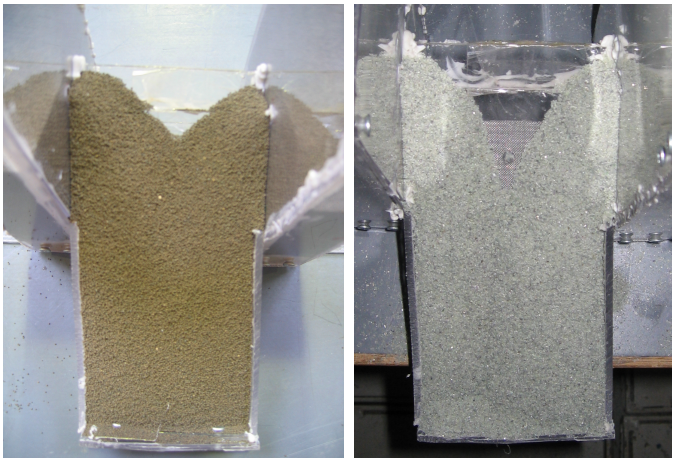

Figure 3.6: First demonstration of filter tray louvers: Left: SB, Right: Olivin

3.3.2 The first assembly design

The 5 components of the assembly are shown in Figure 3.7. All components in Figure 3.7 were made up of Lexan, except Figure 3.7 A which is a metal grid. The

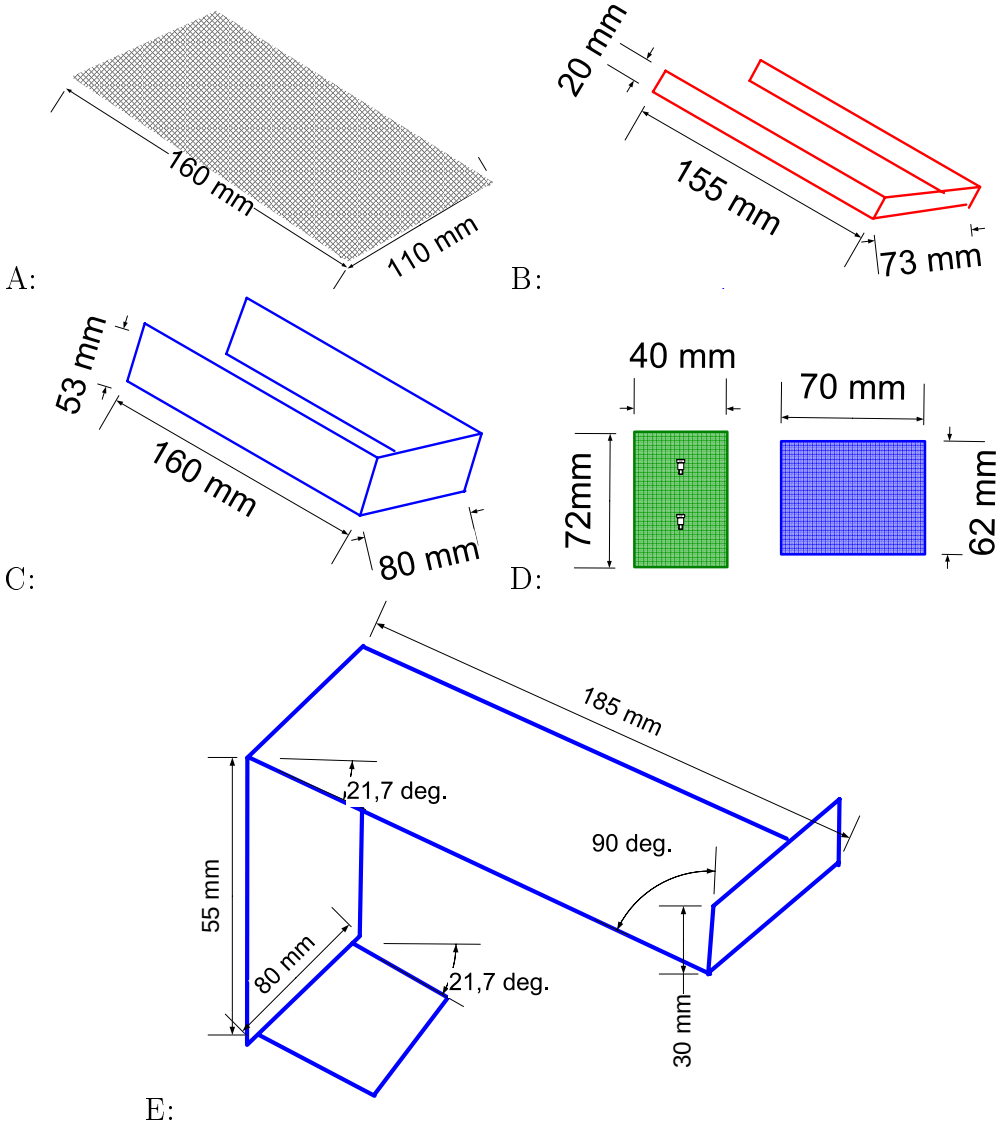

A: Grid, B: Inner frame, C: Outer frame, D: Slide plates,
D: Slide plates E: Assembly plate

Figure 3.7: The components of the first louver design

grid was mounted between the two frames (Figure 3.7 B and C) as shown in Figure 3.8 A, and attached using 6 screws. The slide plate and the support plate (Figure

3.7 D) was placed over and under the grid, as illustrated in Figure 3.8 C. The test assembly had 4 such louvers. Two mounted louvers is illustrated in Figure 3.9. Each louver is attached to the assembly plate with screws in the front, and with piano hinges on the sides. The assembly plate is attached to the next louver with screws.

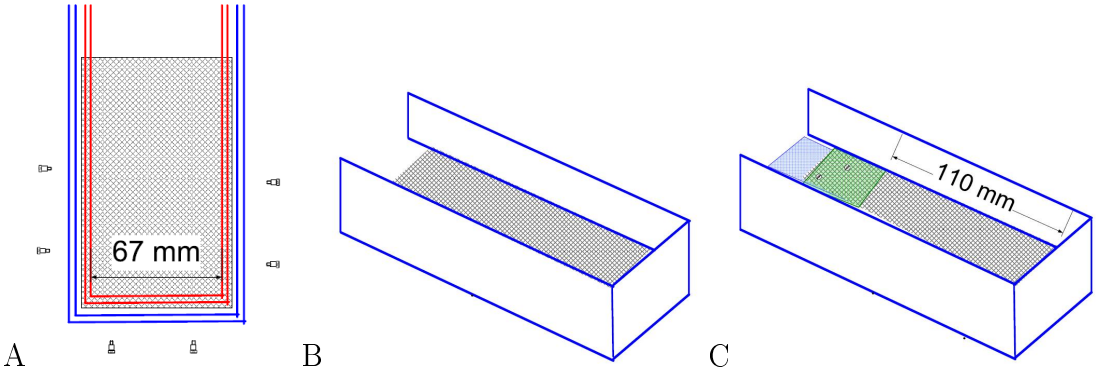

Figure 3.8: The first louver

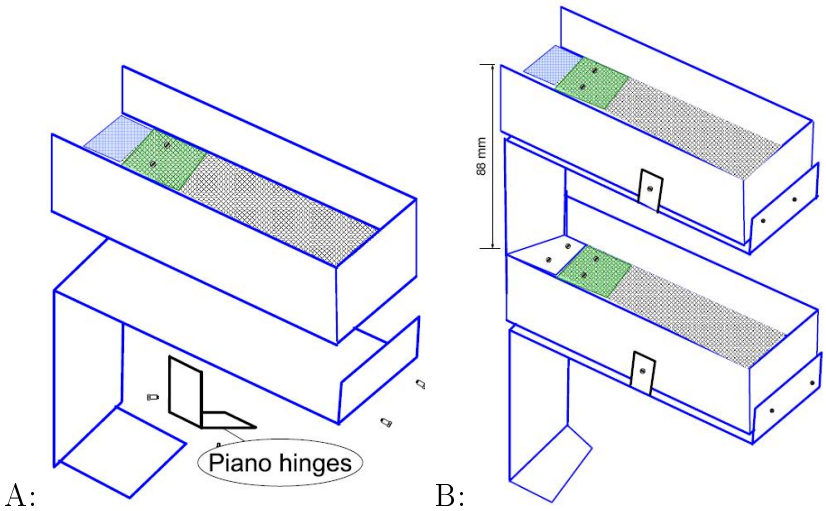

Figure 3.9: The louver assembly

3.3.3 The first filter tray assembly

Four filter tray louvers were built and mounted on a table. Sandfill boxes on either side supplied the louvers with granular medium. Holes were drilled in the table under the sandfill boxes, to allow the filter to be emptied without unmounting the assembly. The cone was mounted as the clean gas duct. The assembly is illustrated in Figure 3.10. The louver angles were adjusted. After the adjustment the angles were measured to be as given in Table 3.2. Circular sandfill openings were drilled through the walls of the sandfill boxes. The holes had a diameter of 10 mm, and were approximately 6 cm from the edge of the grid. The height of the hole above the slide plate is given in Table 3.2. There were variations in both

A:  B: 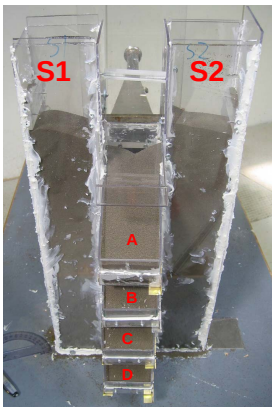

Figure 3.10: The louver assembly, pictures

Louver	Angle	Sandfill hole S1	Sandfill hole S2
A	23°	3,5 cm	4 cm*
B	22°	4 cm	4,5 cm
C	24°	3,7 cm	4,3 cm
D	21°	3,5 cm	4 cm

*) The wall thickness was approximately 10 mm.

Table 3.2: Louver angles and sandfill holes for filter tray assembly

the angle of the louvers and the height of the sandfill holes. The variations were caused by difficulties with machining the lexan plates. Most of the construction was done manually, and the precision was not perfect. The differences in angles and the heights of the sandfill holes, gave the opportunity of testing a range of filter tray louvers, and to find the best louver geometry.

Table 3.2 shows that the angles were approximately the angle of repose for SB. The variations in angle and sandfill hole height resulted in variations in sand bed smoothness. The outer edges of the louvers were shallow for louvers A and D. Louvers B and C had approximately even sand beds of 3 cm.

3.4 Puff back experiments

The objective of puff back experiments was to see that the new design could be cleaned efficiently by puff back. Ideally, the first one or two layers of granular medium should be removed from the louver surface [8]. This equals to from 1,3 to 2,7 kg/m^2, or 11 to 22 grams per louver. The sandspills should be uniform to ensure that dust deposits are removed from the entire louver.

The experiments could not be conducted until the end of June. The delays were caused by other NTNU projects requiring the laboratory resources. Only limited testing of the filter tray assembly has been conducted due to the tight time schedule.

3.4.1 Set-up

The set-up is illustrated in Figure 3.11. Pressurized air from the laboratory grid was used. A pressure reduction valve was used to control the pressure in the tank. Puff back pulses were released through a valve (Festo CPE24-M1H-3GLS 3/8). The valve was controlled by a electrical signal. A Kulite XTE-190 pressure transducer was used to measure the pressure in the cone. The location of the pressure measurement is p1 in Figure 3.11. p1 was located between louver B and C. The pressure in the tank was logged manually. The sand refill of louver A was not working properly, due to thicker walls than for the other louvers. The louver was sealed, and not used during the experiments. Sandspills from each of the three remaining louvers were collected and measured. The signal from the pressure transducer and the voltage signal used to control the valve were sent to a fieldpoint unit and logged.

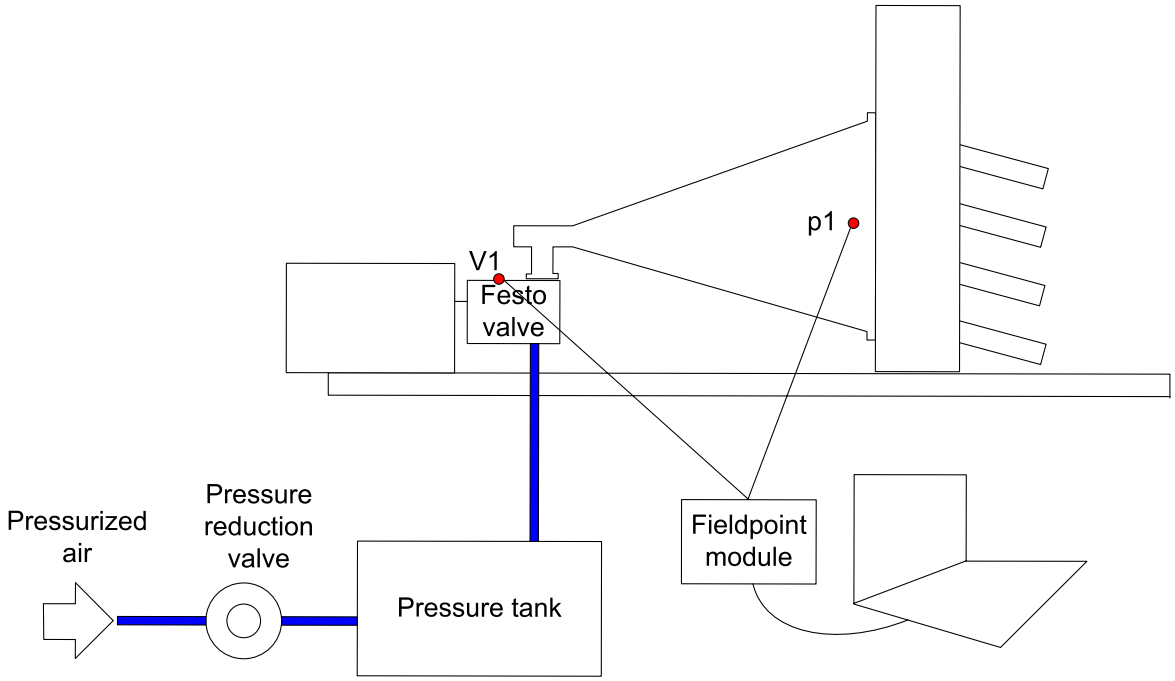

Figure 3.11: Set up for puff-back experiments

3.4.2 Results

Table 3.3 shows the combinations of pressures in the tank and valve opening times tested. The two lowest pressures did not result in any sandspill. Between three and five experiments were conducted for all other combinations. All test results are given on the CD at the end of the thesis.

Pressure in tank (bar)	valve opening times (ms)
2,5	30, 40, 60
2,1	30, 40, 60
1,9	30, 40, 60, 80
1,75	30, 40, 60, 80
1,5	30, 40, 60, 80
1,3	30, 40, 60, 80
1,2	30, 40, 60, 80
1	30, 40, 60, 80

Table 3.3: Puff back experiments performed on the filter tray assembly

Figure 3.12 illustrates the pressure logged just before the filter with 2,5 bar in the tank, with different valve opening times. The maximum pressure is approximately equal for all valve opening times. There is a time lag of about 0,15 s, from the valve opens until the pressure pulse hits the filter.

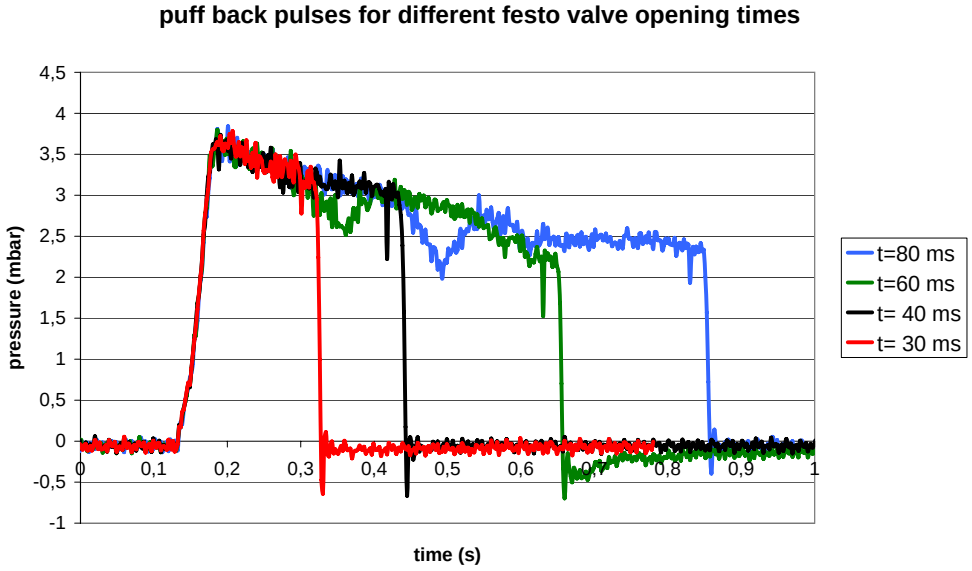

Figure 3.12: Puff back pulses for different valve opening times (p_{tank}=2,5 bar)

Sandspill results for the three louvers are summarized in Figures 3.13, 3.14 and 3.15. Sandspills increased with both pressure and with valve opening time. SB spilled from louver C between puff backs, because the louver was too steep. The bed of louver D was shallow at the outer edge because the louver was not steep enough. Louver B had an even SB bed, and sandspills during puff back only.

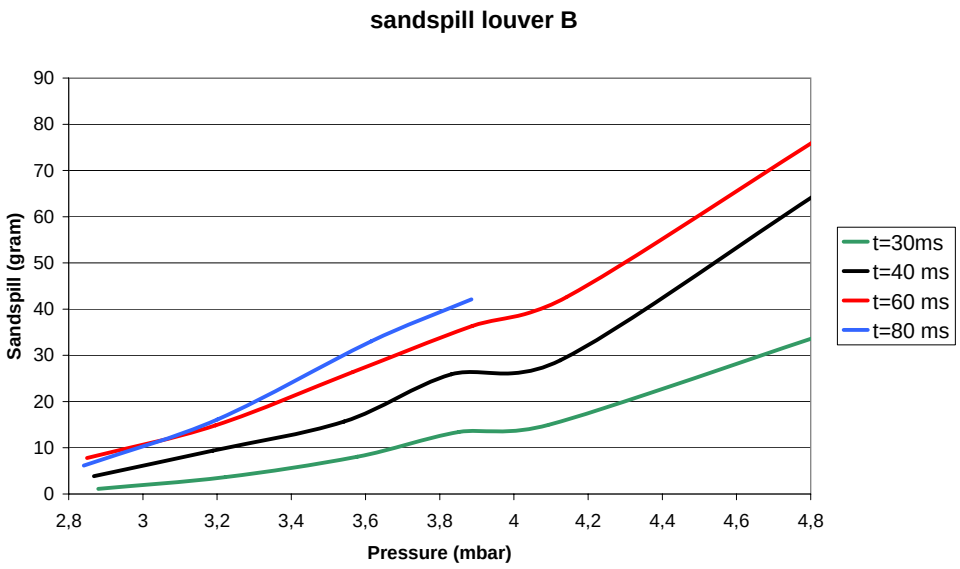

Figure 3.13: sand spills for different pressure measurements and valve opening times, Louver B

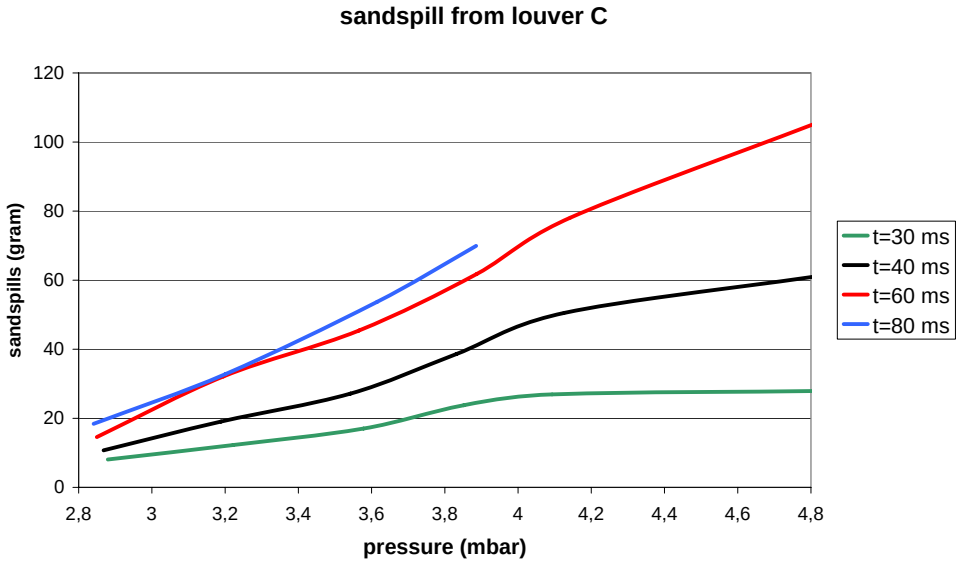

Figure 3.14: sand spills for different pressure measurements and valve opening times, Louver C

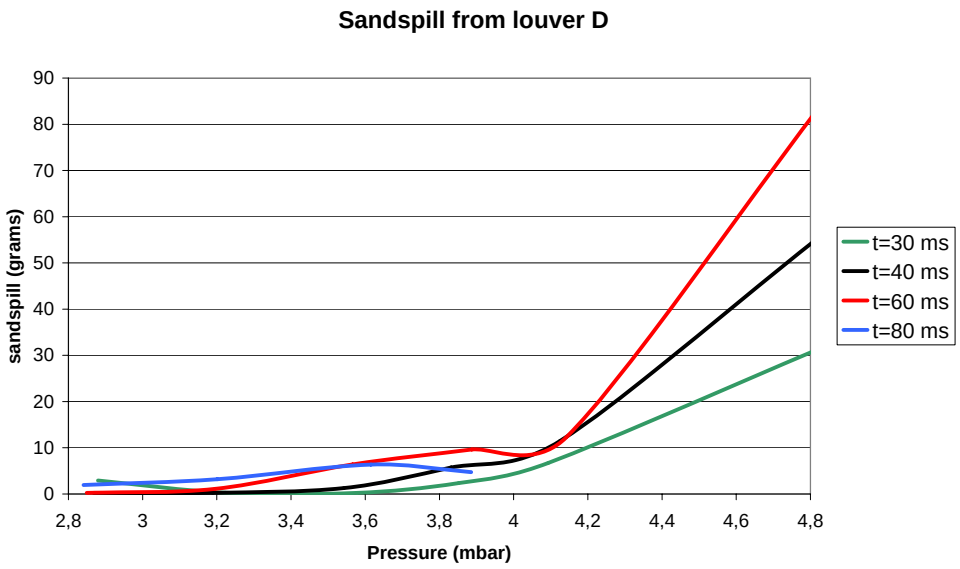

Figure 3.15: sand spills for different pressure measurements and valve opening times, Louver D

3.4.3 Discussion

The pressure was only measured on one location in the cone before the filter, between louver B and C. The pressure distribution just before the filter is assumed to be uniform, and the three louvers are assumed to have been tested under the same conditions. The repeatability in sandspill was good for high pressures and short valve opening times. Sandspill would vary from test to test when the pressures were low and the opening time was long.

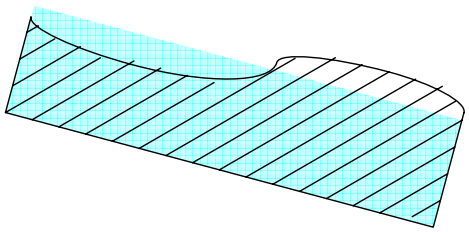

Figure 3.16: SB bed distribution with poor sand refill

The sand refill of the filter tray louvers was not efficient. The sand refill of louver A was found to be inefficient even before the puff back tests, and was

sealed. During experiments, small lexan, silica or wood chips were torn off from the assembly construction, and got stuck in the sandfill holes, causing the SB flow to be slow or to stop entirely. The poor refill caused an uneven bed, as illustrated in Figure 3.16. The puff back gas would blow through only the shallow part of the bed, causing a reduction in the sandspill from the other louvers. The sand refill problem was fixed by sticking something through the holes to re-open them. The problem could be avoided by making sandfill holes larger or using more rigid materials in the construction.

The three filter trays had different amounts of sandspill. The cause of the variations is believed to be the difference in the geometry. Louver C was the steepest bed, with an angle of 24 °. The louver had a uniform, stable bed before puff back tests were initiated. After the puff backs the porosity had changed, and SB would spill from the louver at any movement or vibration. The angle of louver C was found to be too steep. The SB bed in louver D was shallow at the outer edge before the puff back tests. The SB distribution did not improve during the experiments, and the angle (21 °) was found to be too low. Louver B was found to be the best filter tray louver, with a louver angle of 22 °. The bed was uniform, and there were no sandspills between puff backs.

The activation pressures were different for the three louvers due to the geometric differences. The activation pressure of louver C was found to be near zero, as SB would spill at any movement. The activation pressure of louver D is found from Figure 3.15. The curves for the different valve opening times bend upwards between 3,8 and 4 mbar. The activation pressure is approximately 3,9 mbar. There were sandspills with pulses below this pressure, mostly when the valve opening time was long. There is a clear increase in the effect of the pressure above 3,9 mbar.

The activation pressure for louver B was more difficult to find. The curves in Figure 3.13 has no clear bend upward, and instead they rise evenly. The activation pressure was estimated to be 3,25 mbar. The estimation was done by prolonging the tangential lines from the range of ideal sandspill (between 11 and 22 gram) illustrated in Figure 3.17.

The activation pressures found are very low compared to the activation pressures found in the works of Risnes [4] and Lee [1]. The low activation pressure may partly be explained by the more shallow beds. The lack of a clear activation pressure may be explained by the angle of the louvers. For earlier PBFs, the angle of the louvers have been two to three degrees below the angle of repose [11], while the angle of louver B is the angle of repose. Very slight movement of will cause SB to start sliding. We believe it is advisable to keep the filter tray louvers as close to the angle of repose as possible to ensure an even sand bed. Uneven sand beds seemed to cause uneven sandspills. The puff back gas would flow through the

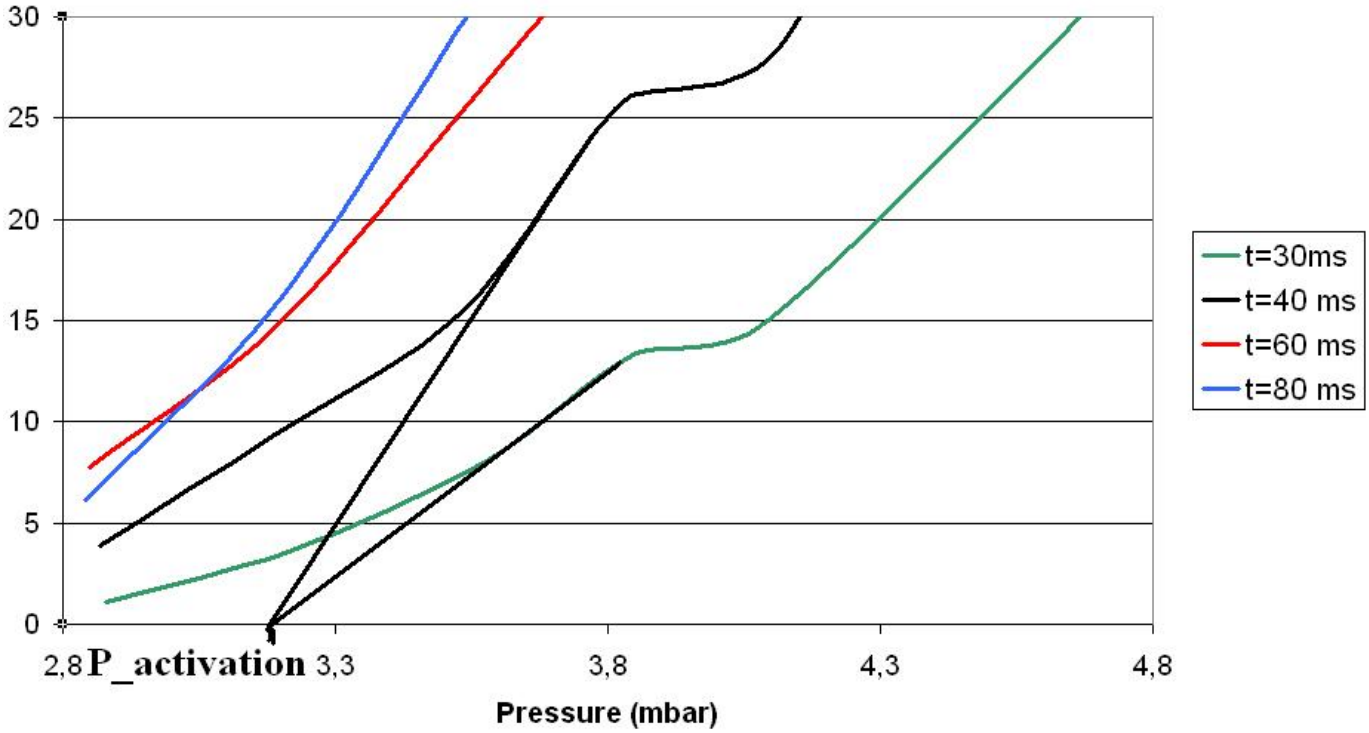

Figure 3.17: Approximation of activation pressure for louver B

more shallow parts of the beds, causing less sandspill in the deeper parts of the beds. (For these experiments, this was only a problem when sandfill holes were clogged.)

We believe that the steep angle of the filter tray louvers reduce the importance of the activation pressure. Even puff back pulses with very low pressure can cause a small amount of sandspill. The sandspills would increase evenly with both pressure and with the length of the puff back pulse.

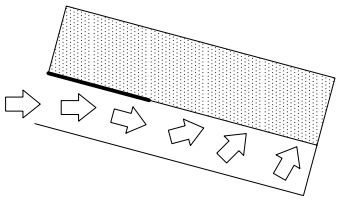

Figure 3.18: Direction of puff back pulse for filter tray louvers

In earlier experiments (Risnes [4], Lee [1] and Stanghelle [2]) the puff back

pulse have hit the louvers from the side, while the shape of the filter tray louvers lead the puff back pulses to hit the bed from below as illustrated in Figure 3.18. With the difference in the direction of the puff back pulse, the mechanisms of the sandspills from the filter tray louvers may be very different than the mechanisms in a regular PBF. The mechanisms of the sandspill should be investigated. The sand spill mechanisms can be captured with a high speed camera.

All experiments were performed on clean filter tray beds.

3.5 Improvements to the design

Most of the suggestions for improving the filter tray design, are measures to reduce the area ratio, described in section 2.5. The louver angle should be 22 °, as for louver B. The clean gas geometry should be optimized for efficient puff back cleaning. Due to lack of time, the optimization of the clean gas volume (illustrated in Figure 3.19) is left for future work.

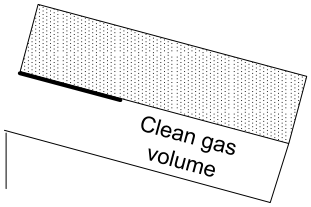

Figure 3.19: The clean gas volume

Measures to increase the area ratio Θ

- The height between the modules can be decreased. The prototype was designed considering the possibility of using both SB and Olivin. Therefore, the space left open for sandfill holes were over-dimensioned. The louver height can be reduced to 6,5 cm, increasing area ratio Θ from 1,36 to 1,7.
- The slide plate may be shortened to increase the filtration area. During experiments, the SB bed looked uniform approximately three centimeters from the sandfill holes. Puff back experiments with different slide plate lengths should be made to determine the minimum length.
- The slide plate can be shaped as a V, illustrated in Figure 3.20. This could increase the filtration area. The slide plate only needs to cover the part of the louver, not covered by the granular medium. Tests should be performed to see if sandspills with the V-shaped slide plate are uniform.

- The length of the louvers can be increased. Puff back tests with different louver lengths should be performed. Longer louvers give larger filtration area and a greater area ratio Θ. If the louver is too long, the granular medium may not spill from the entire louver.

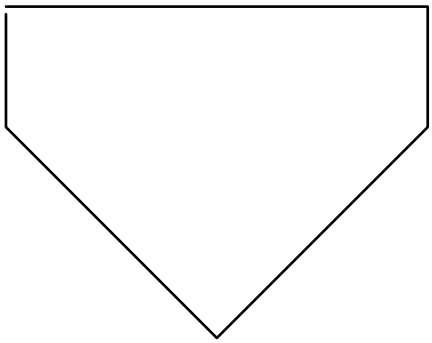

Figure 3.20: V-shaped slide plate

Measures to optimize the clean gas volume The shape of the clean gas volume determines the flow of the puff back pulse, and the sandspill. The filter tray louvers that have been built had cubical clean gas volumes with a height of 2 cm. Decreasing the height of the clean gas volume, would reduce the nominal face area and increase the area ratio Θ. A very small clean gas volume may reduce sandspills, or cause uneven sandspills, because the gas will always chose the path of least resistance. Therefore, puff back experiments with reduced clean gas volume should be performed.

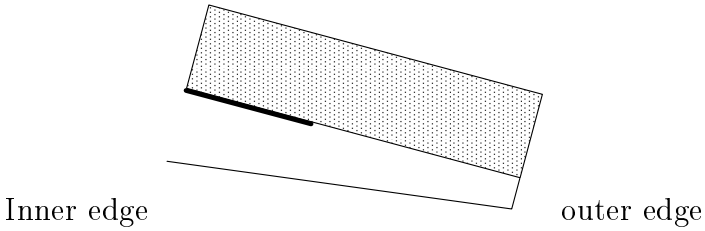

Figure 3.21: Filter tray louver with decreasing clean gas volume

The shape of the volume can be changed. The intensity of the puff back pulse will decrease as moving into the clean gas volume, because the energy will be used

for moving the granular medium. The pulse hitting the bed at the outer edge will be weaker then the pulse hitting the inner part of the louver. By reducing the flow area for the pulse in the outer part of the clean gas volume, as illustrated in Figure 3.21, the pressure may be increased at the outer edge of the filter.

Miscellaneous measures The sandfill holes should be larger. The flow of granular particles was very sensitive to contaminants in the granular medium due to the small holes.

Chapter 4

Design of an industrial panel bed filter

4.1 Introduction

In this chapter, a hypothetical gas cleaning system for a district heating plant is presented. The system is illustrated in Figure 4.1. Biomass is combusted, and the

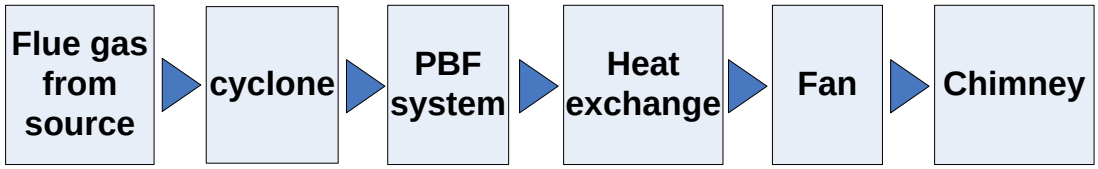

Figure 4.1: Block diagram of complete PBF system

heat in the flue gas is to be used for district heating. Particles are to be removed prior to the heat exchange, to avoid the risk of dust and unburned components clogging the heat exchanger and damaging the fans. The PBF technology is of interest, because of its resistance to high temperatures and to the various contents in the flue gas. An entire PBF system, apart from the fan and the heat exchanger, has been designed. The coarse fraction of the dust particles will first be removed in a cyclone. The rest will be removed in the PBF before the clean gas is led through a heat-exchanger and a fan. The clean, cold flue gas is released through the chimney.

4.1.1 Design criteria

The inlet gas characteristics are found in Table 4.1. The biomass is combusted using air as the oxidation agent. The real flue gas volume flow resulting from the data in Table 4.1, was found to be 42 927 m^3/h. The PBF and the entire PBF

Characteristic	value	
Gas temperature at inlet	450	°C
Volume flow	20.000	Nm^3/t
O_2 per mole dry air	7,5	%
Steam per mole dry air	20	%
Dust concentration per volume dry air	450	mg/Nm^3

Table 4.1: The inlet gas characteristics

system will be designed for two nominal face gas velocities; 0,1 and 0,2 m/s.

4.1.2 Particle emissions from biomass combustion

Particle emissions can form aerosols which are tiny particles of solid or liquid present in a gas. The particle emissions can have a negative effects on the human respiratory system [12], and are considered pollutants. Emissions from biomass combustion can be divided into two groups [12]; emissions from complete and from incomplete combustion. Particle emissions are included in both groups. The emissions from complete combustion are mainly fly ash resulting from entrainment of ash particles in the flue gas and salts that come from reactions between sulphur, calcium, natrium and chloride. The particle emissions from incomplete combustion can be [12]:

- Soot consisting of mainly carbon. The soot is the result of local lack of oxygen in the flame zone or from local flame extinction.
- char particles that follow the flue gas flow due to low specific density.
- condensed hydrocarbons (tar) resulting from low combustion temperatures, too short residence time in the combustion chamber or from the lack of oxygen.

Particle emissions from biomass combustion plants can be reduced by optimization of the combustion chamber [12]. Due to the diversity of particle emissions, flue gas filtration is utilized in large scale biomass combustion plants.

4.1.3 Requirements and conditions

The energy is to be used for district heating, and a goal will be to keep the temperature high and to minimize heat loss. The entire system should be heated and insulated, to preserve as much of the energy as possible. Another goal is to keep the design compact. A large design with long pipes and a great surface area will have greater heat loss, than a more compact system.

4.2 The cyclone

The cyclone is a device for removing particles from a gas flow [3]. Compared to the PBF or to fabric filters, the operation of a cyclone is very simple. The cyclone has no moving parts, and both operational and investment costs are low. The reverse flow vortex cyclone, illustrated in Figure 4.2, is most commonly used [2]. Gas enters the cyclone body tangentially, and causes a strong vortex flow. Particles are influenced by centrifugal forces, and move radially toward the cyclone walls. The direction of the flow is reversed in the bottom of the cyclone, and clean gas exits at the top. Particles close to the cyclone walls are forced out of the flow by gravitation and by the outer vortex flow. Particles exit in the bottom [2].

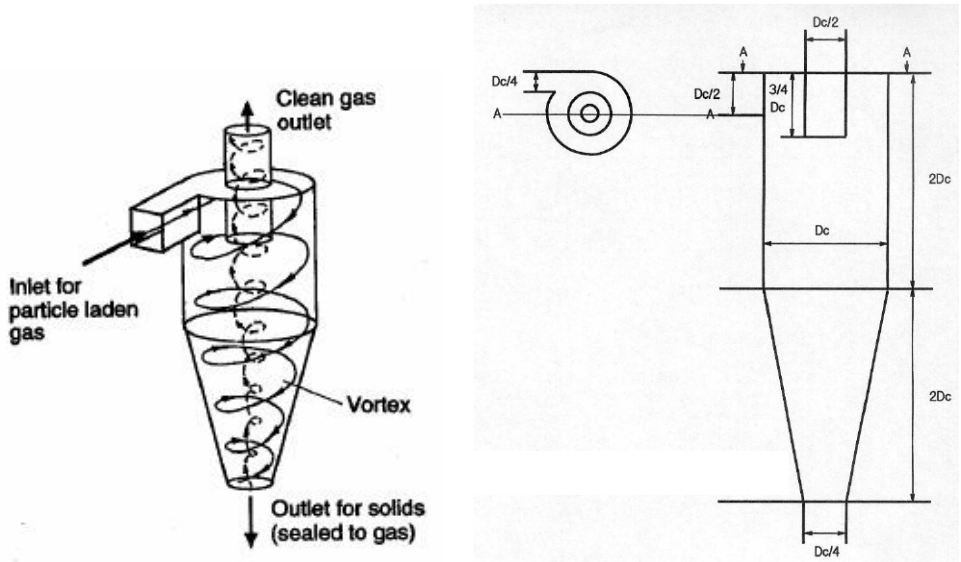

Figure 4.2: Left: The flow pattern of a reverse vortex cyclone [2] Right: The cyclone design. [6]

The cyclone design in this work is an upscale of the cyclone used in the BioSOFC-project, illustrated in Figure 4.2. The critical separation diameter d_c

and the geometric length D_c in the Figure 4.2 are used as design parameters. The relation between critical separation diameter d_c, D_c and the gas flow is described by equation 4.1. Ideally, all particles with diameter larger than d_c are in the coarse fraction, while the smaller particles are in the fine fraction exiting the cyclone with the gas stream [6]. The BioSOFC cyclone design had a critical separation diameter of 1,7 μm.

$$d_c = \left(\frac{9D_c^3\mu 3600}{64\pi VN(\rho_p - \rho_f)}\right)^{\frac{1}{2}} \tag{4.1}$$

μ is gas viscosity, ρ_p and ρ_f are particle and gas densities. V is the volume flow, and N is the number of gas rotations in the cyclone.

Equation 4.1 describes ideal separation, but cyclones are not ideal devices. The separation efficiency can be calculated if particle distribution is known. Separation efficiency is made up of two terms; Θ_e describing separation due to particle loading exceeding the maximum loading of a cyclone, and Θ_i due to separation in the cyclone gas flow (vortex separation) [3]. The relation between Θ_i, Θ_e and the total efficiency Θ_{total} is expressed in Figure 4.3 and in equation 4.2:

$$\Theta_{total} = \Theta_e + \Theta_i \frac{\mu_G}{\mu_e} \tag{4.2}$$

Where μ_G and μ_e are outlet and inlet dust loads. The outlet dust load can be calculated from inlet dust load and critical particle diameter [3]:

$$\mu_G = 0,025 \frac{d_c}{d_{50}} [10\mu_e]^{0,15+0,66exp[-\frac{\mu_e}{0,015}^{0,6}]} \tag{4.3}$$

d_{50} is the median particle size in a particle distribution.

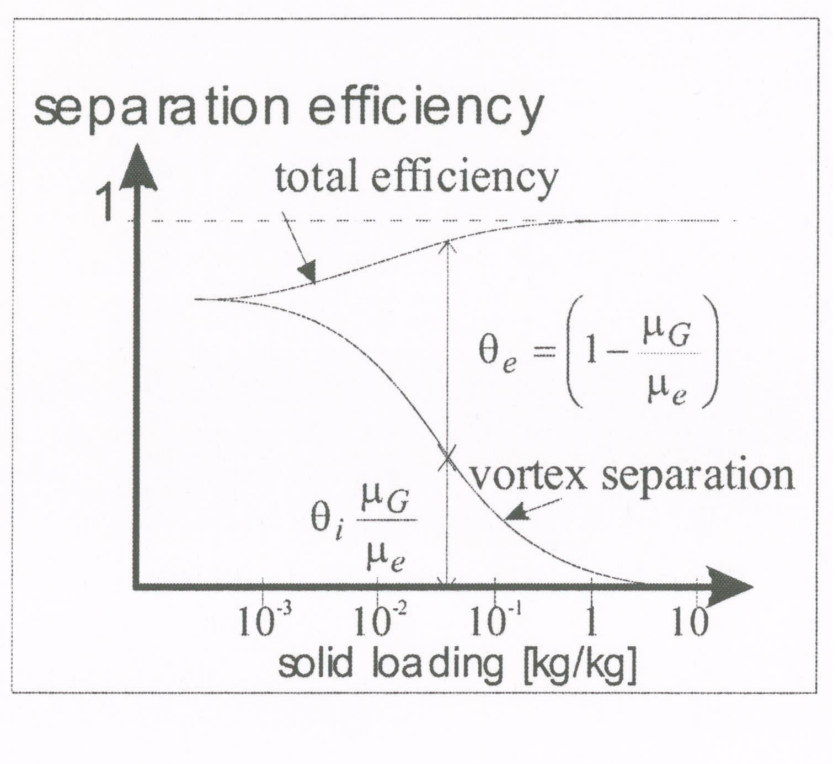

Figure 4.3: Separation efficiency [3]

The particle distribution for biomass combustion is unknown, and may vary depending on the biomass and the combustion chamber. The cyclone will be designed when a particle distribution for the plant is available.

Design decision: *The cyclone efficiency is set to 95 %.*

4.3 The PBF system

95 % of the dust in the flue gas will be removed in the cyclone. The gas entering the PBF system will have a dust concentration of 23 mg/Nm^3 (10,7 mg/m^3). With a gas flow of 20.000 Nm^3/h, 460 grams of dust enters the filter every hour.

4.3.1 Choice of granular medium

Several granular mediums of are commercially available. Due to lack of experience with other granular mediums, only Olivine and SB (Appendix A) were considered for this design.

The angle of repose is quite low for SB, due to a high sphericity. The louvers are less steep. SB has a high crush resistance compared to most metals. The hardness of SB can cause problems because equipment such as screw feeders are torn.

Olivine particles are angular and irregular. The angle of repose is larger, and the material is not as resistant to stress as SB. Broken Olivine particles form dust, and can follow the clean gas flow.

Design decision: *SB is chosen due to its resistance to stress.*

4.3.2 Filter design

The filter tray louvers The filter tray louver design resembles the design described in section 3.1.3. The width of the filter tray louvers will be increased to 0,5 m. The length of the louver will be 0,1 m, as in section 3.1.3. The length of the filtration area for one louver was measured to be 0,12 m. The height of the nominal face area was measured to be 0,088 m. This gives an area ratio of 1,36. However, the height of the nominal face area can be reduced to 0,065 m per louver as described in section 3.5. The reduction gives an area ratio of 1,7.

Design decision: *Filter tray louvers with an area ratio of 1,7, will be employed.*

Alternative module designs The height of the modules should be 3 m, and the number of louvers in each module was found using the nominal face area:

$$NumberOfLouvers = \frac{3m * louverwidth}{NominalFaceArea/louver} = \frac{3m * 0,5m}{0,065m * 0,5m} = 46 \tag{4.4}$$

There are countless ways of arranging the PBF modules, limited only by the inventiveness of the designers. The arrangements considered are shown in Figure 4.4. The cubical modules are double-sided, and 5 such modules are illustrated in Figure 4.4. The modules of the circular design are single-sided. Each module circle consist of 10 modules sharing one circular clean air duct.

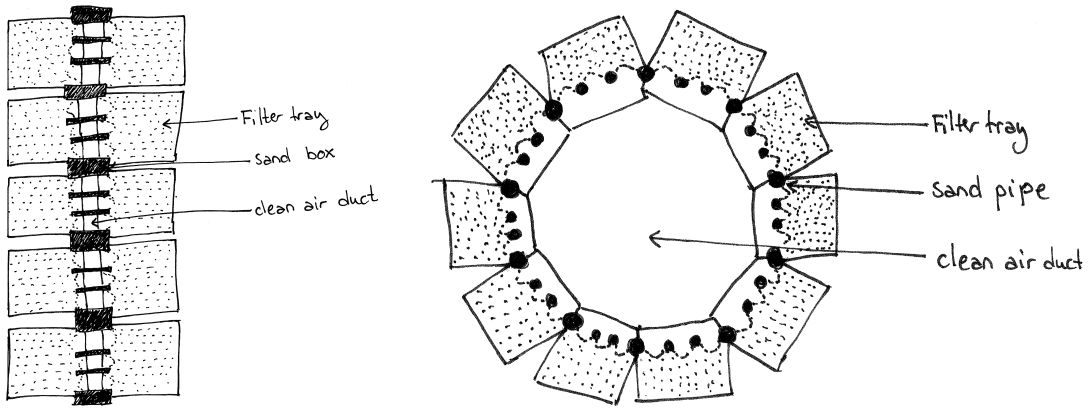

Figure 4.4: Filter tray module arrangement; Left: Cubical design Right: Circular design

Module arrangement and spacing Two different PBF system designs are made, for the two nominal face gas velocities considered: 0,1 and 0,2 m/s. Table 4.2 shows how these nominal face gas velocities affect the filter design. The number of filter modules must be an integral number. To ensure that the nominal face velocity do not exceed 0,1 and 0,2 m/s, the number of modules have to be rounded up.

Propositions for module placement are shown in Figures 4.5 and 4.6. The illustrations are not scaled, and can not be used to determine what design will be the most space efficient.

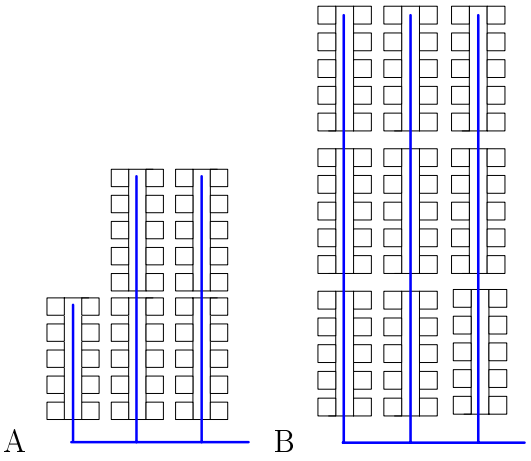

Figure 4.5: Filter module arrangement, cubical design. Left: 0,2 m/s Right: 0,1 m/s

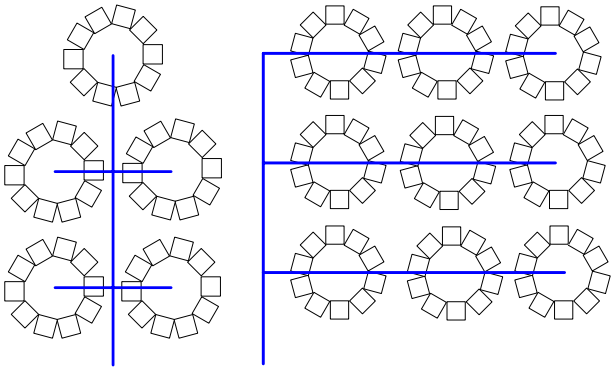

Figure 4.6: Filter module arrangement, circular design. Left: 0,2 m/s Right: 0,1 m/s

Filtration velocity	0,1 m/s	0,2 m/s
Requisite nominal face area	133 m^2	67 m^2
Requisite number of filter modules		
Cubical design	45	23
Circular design	89	45

Table 4.2: Calculations of filtration area and requisite number of filter modules

The cubical module columns were placed in rows of three. The clean gas pipe was placed parallel to the column rows, above. The suction pressure in the clean air duct will vary depending on the distance from the gas collection pipe. Variations in pressure will cause variations in gas flow through the modules, and velocities may exceed design values. Gas collection from several points in each column is necessary to ensure approximately uniform pressure distribution. Gas from the three rows is collected in a manifold as illustrated in Figure 4.5.

Using the circular arrangement, the clean gas from each module circle is collected from one point in the center. The pipe arrangement for a gas velocity of 0,1 m/s has similarities to the pipe arrangement for the cubical design, with three gas pipes collecting gas from three circles each. The clean gas from the three pipes is collected in a manifold. The gas collection for a velocity of 0,2 m/s could be done in the same way. However, the filter system will be more compact if piping is done as shown in Figure 4.6, and each module circle has an individual clean gas pipe.

Space considerations The columns of Figure 4.5 are approximately 2,5 meters long and have a width of approximately 0,7 m. The module circles of Figure 4.6 have a diameter of 2 m. The spacing between the units of both designs should be sufficient to prevent the transfer of fly ash between units during cleaning. If dust is blown on to the next unit during cleaning, the cleaning will be less efficient and the active filter area will be reduced. Dust cake from the top louvers will still be efficiently removed. The pressure drop over the top louvers will therefore be considerably lower than for the louvers with dust cake. This difference in pressure drop can cause gas velocities to exceed the design values through the top louvers, because gas flow will choose the path of least resistance.

The spacing between units is chosen to be 0,6 m based on an early PBF system design made by Squires [1]. The value can probably be reduced, but experiments examining sandspill during puff back cleaning should be performed first. Table 4.3 show the results from an estimation of the area required for the two module arrangements. The circular design will acquire approximately double the space of the cubical design.

	U_s=0,1 m/s	U_s=0,2 m/s
Circular design	55 m^2	35 m^2
Cubical design	30 m^2	20 m^2

Table 4.3: Comparison of filter module footprint for different module designs and U_s.

A more spacious module design, will lead to a bigger enveloping house and longer pipes. A greater the surface area, result in greater heat loss.

Design decision: *The cubical module design is applied to the PBF system. The module arrangements are illustrated in figure 4.5. The spacing between the module columns were set to 0,6 m.*

Module column design The exact size of the module columns are determined by

- the number of modules in each column
- the clean gas area
- the required slide area
- and the space required for sand refill

The clean gas area is directly linked to the gas velocity in the clean gas duct. The gas speed in earlier designs had to be kept low due to the risk of sand spills into the clean air duct. The old designs had back louvers. High gas velocities could cause fluidization of the granular medium. Sand in the clean air duct will not be a problem using the filter tray design, as there is a grid between the granular medium and the clean air duct. However, the risk of dust penetrating the filter increases with the gas velocity.

The gas velocity in the clean air duct should around 2 to 3 m/s [11]. Keeping the gas velocity below 3 m/s is important to avoid dust in the clean air pipe. A low gas velocity will not cause any problems, but the space required will be increased. Using this information, calculation examples of required clean gas duct area were made, and are given in Table 4.4.

An area of 1 m^2, give gas velocities below 3 m/s for (U_s=0,2 m/s). The duct area is slightly over-dimensioned for (U_s=0,1 m/s), and the gas velocity in the clean air duct will be below 2 m/s. Only one standard PBF module design is made for simplicity.

Design decision: *The clean gas duct area is set to be 1 m^2. Exact, horizontal measurements for the module column design are given in Figure 4.7.*

	(U_s=0,2 m/s)	(U_s=0,1 m/s)
volume flow [m^3/s]	3	1,5
Required duct area, gas velocity = 2 m/s [m^2]	1,2	0,7
Required duct area, gas velocity = 3 m/s [m^2]	0,8	0,4

Table 4.4: Calculations of clean gas duct area

Each louver in the module column design (Figure 4.7) has 4 sandfill boxes; one on either side shared by neighboring louvers, and two cutting through the louvers. Each sandfill box is 6 cm wide. The space between louvers is set to 2 cm. The length of the tilted louver is 18,5 cm, corresponding to 17,2 cm in horizontal projection. The entire row will be 262 cm long and 72,4 cm wide.

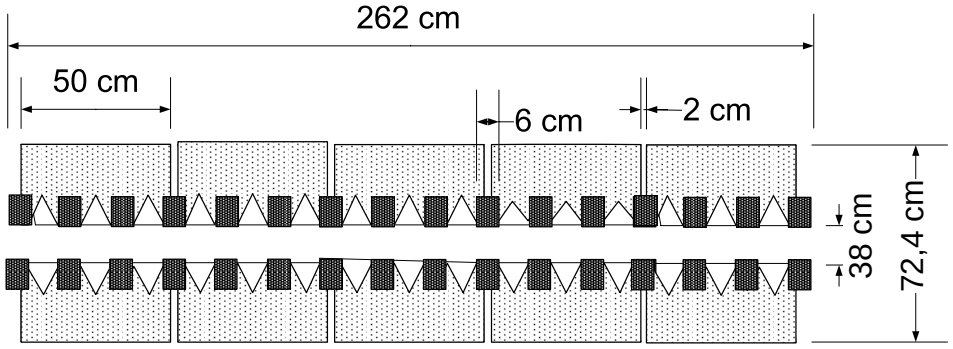

Figure 4.7: Module with exact horizontal measurements

4.3.3 Enveloping house

The PBF modules are placed in an enveloping house, like the one illustrated in Figure 4.8. The space between the modules and the walls of the enveloping house is set to be 60 cm. The footprint of the enveloping house is

- 7,896 m * 2,19 m (U_s= 0,1 m/s)
- and 5,264 m * 2,19 m (U_s= 0,2 m/s)

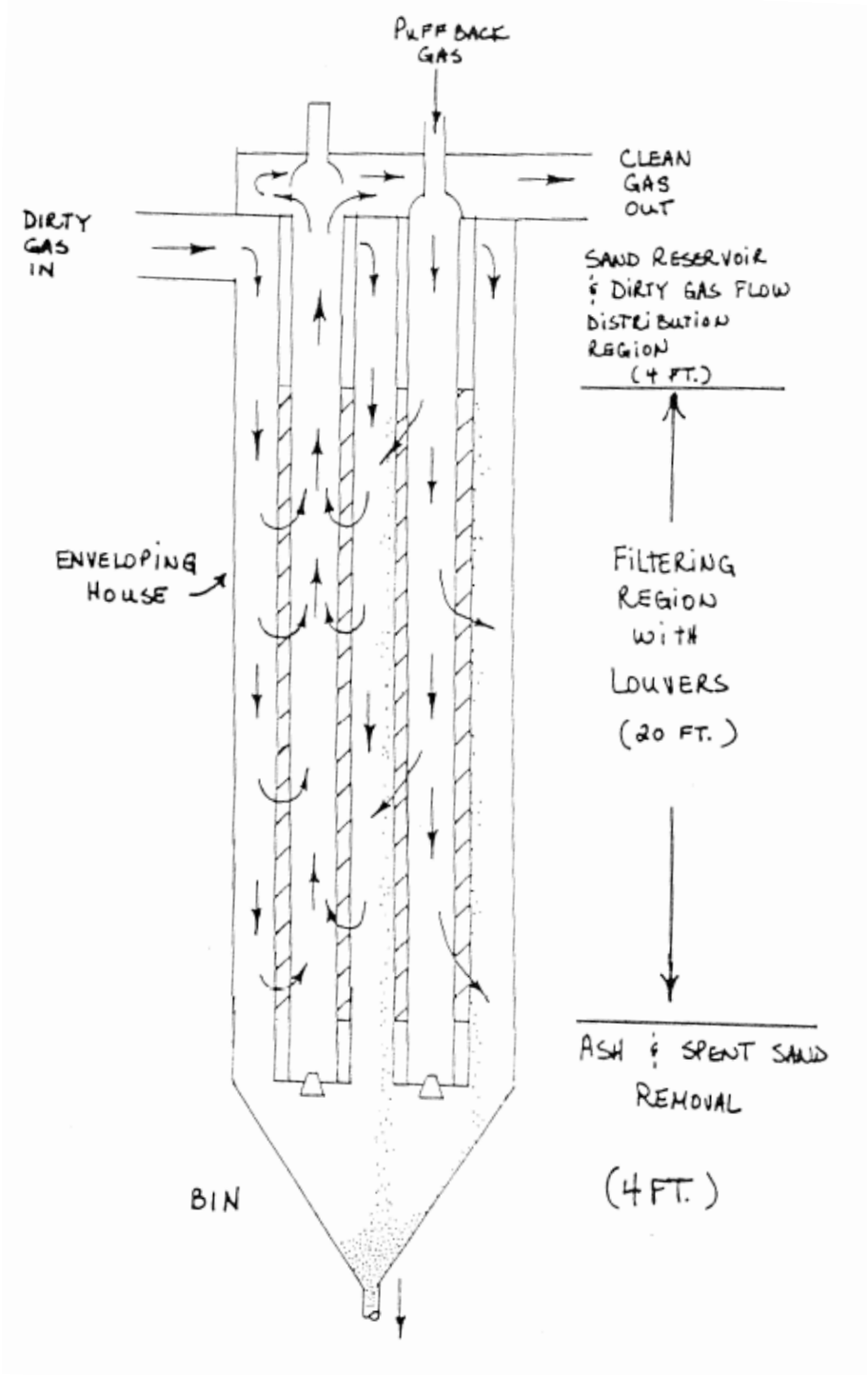

Figure 4.8: PBF in envelope house [1]

The floor of the enveloping house is angled, and sand spills from puff back cleaning are collected in bins. To ensure that the sandspill slides to the bin, the wall angles have to exceed the angle of repose for SB (21,7 °). A large angle will increase the height of the enveloping house. The angles are set to be 25 and 29 °. The height of the enveloping house can be reduced by increasing the number of bins as illustrated in Figure 4.9:

- One bin gives a floor height of 1,83 m
- Three bins give a floor height of 0,61 m

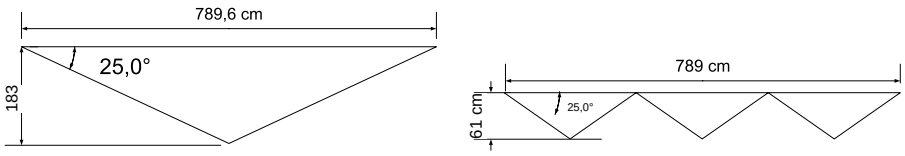

Figure 4.9: Cross section of the bottom of the enveloping house U_s=0,1 m/s, Left: One bin Right: Three bins

There will be three (U_s=0,1 m/s) and two (U_s=0,2 m/s) bins at the bottom of the enveloping house. The angles of the floor will be 25 and 29 ° giving a floor height of 0,61 m.

The floors are illustrated in Figure 4.10 A and B. The enveloping house for U_s=0,2 m/s could be smaller, as illustrated in Figure 4.10 C. The design in Figure 4.10 B was chosen due to its simplicity.

Gas will enter the enveloping house through one pipe from the side in the top region of the enveloping house. Inevitably, the gas inlet will be closer to some modules than to others. The difference in distance may cause variations in gas flow, and modules opposite to the gas inlet may be unused. To prevent uneven gas flow, and to ensure that all modules are functional, gas must be dispersed.

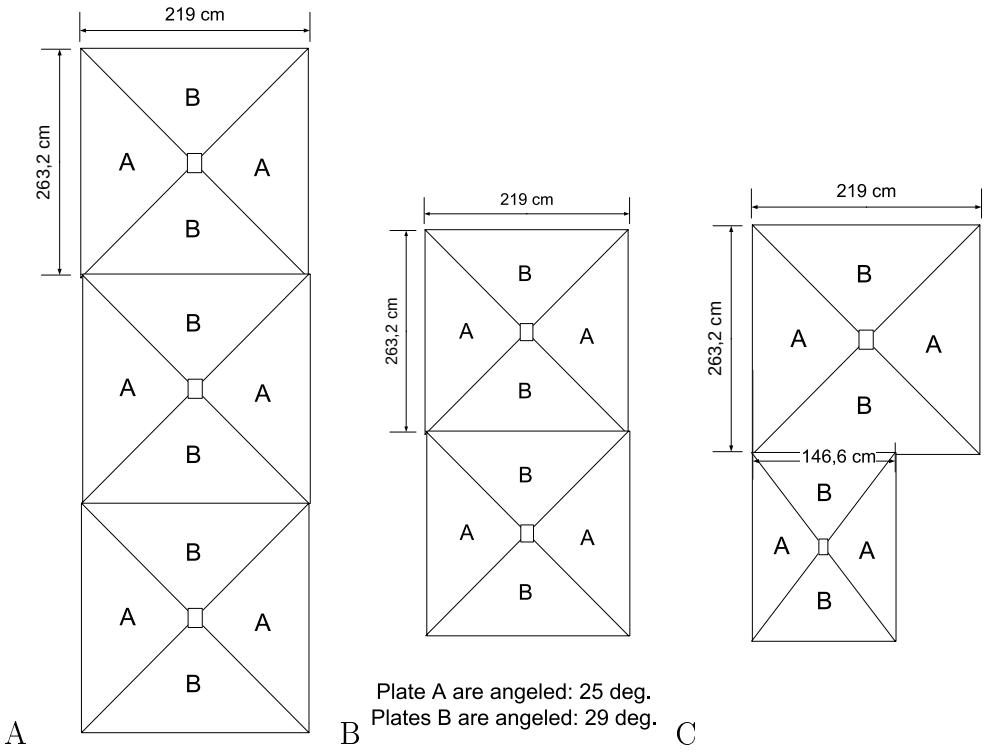

Figure 4.10: The floor of the enveloping house for gas velocities A: 0,2 m/s B:0,1 m/s (Over-dimensioned) C:0,1 m/s (minimum area)

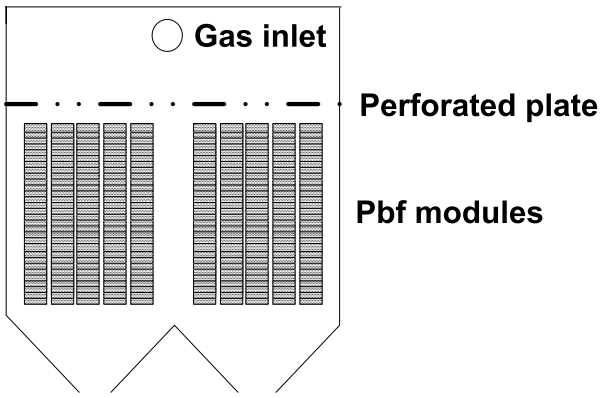

Figure 4.11: The enveloping house design

Two means (illustrated in Figure 4.11) are employed:

- A volume will be left open between gas inlet in the top above the PBF modules. The sudden expansion in flow area will cause a reduction in gas velocity.
- A perforated plate will be installed between the gas inlet and the modules. If fluid motion in the volume above the perforated plate is small, the volume can be considered a gas reservoir. The flow through the holes in the perforated plate will be equal if the pressure distribution is in the reservoir is even. The gas will be dispersed.

4.3.4 Puff back system

Puff back control system The puff back system can be controlled by two alternative methods [13].

1. Pressure drop is measured over each module, and puff back is initiated automatically for each module at a predetermined pressure drop.
2. Pressure drop is measured over the entire filter installation. At a predetermined pressure drop the puff back process is initiated. The modules are puffed in a fixed sequence, with a predetermined time lag between each puff back.

Using the first method will allow controlled pressure drop over each individual module at any time. However, the method requires more pressure measurements and will therefore be more expensive [13]. The second method is simpler, and requires less equipment.

Design decision: *The puff back will be initiated when the pressure drop over the entire filter reaches a predetermined value. All the module columns will be cleaned in a fixed sequence, with a predetermined time lag.*

The process should be optimized though experimentation.

Cycle time and pressure drop On-line measurements of pressure will be used to determine when puff back should be initiated. The best maximum pressure drop will be determined by calibration. The puff pack pressure and the cycle time of the system determines the amount sandspill, which is an important input parameter for the design of a sand recycle system. Therefore, assumptions about the pressure drop and the puff back cycle time is made.

Experiments conducted by Håvard Risnes [4] was used as a basis for the puff back system design. The Risnes filtration tests were performed on a PBF with L10-56 louver design. The pressure drop over a PBF with filter tray louvers is believed to be less than with L10-56 louvers. No experiments have been conducted with the filter tray louver, and the pressure drop is assumed to be similar to the pressure drop in the Risnes experiments, with a ΔP_{max} ranging from 1200 to 2000 Pa.

The puff back cycle times were assumed to be one hour and 30 minutes (U_s= 0,2 m/s) and three hours (U_s= 0,1 m/s). The puff back pulse should remove the two topmost layers of the filtration medium [14]. Each module column has a filter surface area of 23 m^2. For each puff back cycle between 30 and 62,1 kg of SB is removed from each module. For the entire PBF system, this sums up to between 100 and 207 kg/h (U_s= 0,2 m/s) and between 90 and 186,3 kg/h (U_s= 0,1 m/s).

Puff back system arrangement When the modules are cleaned, the clean air flow will be stopped, and a pressure pulse will be released in the opposite direction. One module column will be cleaned at a time. The pulse should hit the filter trays from above, and there should be at least one puff back outlet directly above each module. Ideally the pressure pulse should have a high pressure and short time span [1].

A good puff back pulse can be achieved by releasing the pulse from a pressure reservoir using high-speed valves as illustrated on the left in Figure 4.12. A gas pipe can be a pressure reservoir if the diameter is large, and flow is slow. If the pressure distribution in the reservoir is even, the flows through the reservoir outlets are equal.

Another alternative puff back arrangement is illustrated on the right in Figure 4.12. The entire PBF column can be regenerated simultaneously using one valve connected to a pressure source. The valve will have to have a greater diameter. There should be outlets over each module. This method will be cheaper due to the space efficiency and the reduction in number of valves.

Both methods illustrated in Figure 4.12 are feasible. The first method, using the high-speed valves may result in more efficient regeneration due to a better control of the puff back pulses. The method is more expensive due to the cost of the high-speed valves. The puff back arrangement on the right in Figure 4.12 is simpler and cheaper because less equipment is required.

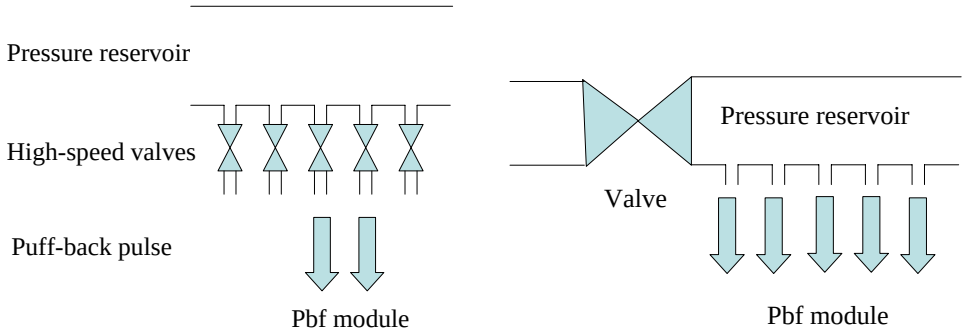

Figure 4.12: Puff back system arrangements Left: high-speed valves and pressure reservoir Right: One valve and pressure reservoir

Design decision: *The puff back arrangement is illustrated in figure 4.12. The puff back pulse is released through one high speed valve, into a puff back pipe with several outlets over each module.*

The puff back outlets cannot be directly above the louvers. The pressure pulse needs space to spread out, so that the entire louver is hit by the pulse. The spreading of the the pulse is described by equation 4.5 [8] and Figure 4.13. x is the vertical length, $D_{louvers}$ and D_{outlet} are the width of the louvers and the diameter of the puff back outlet, respectively.

$$x = \frac{D_{louvers} - D_{outlet}}{2sin(\frac{\beta_d}{2})} \tag{4.5}$$

β_d is the angle of divergence. For $\frac{x}{D_{outlet}}$<100, β_d=20° according to [8]. Using one, one inch puff back outlet over each louver, the distance x have to be more than 130 cm. Using two outlets, the $D_{louvers}$ can be halved and the new minimum distance x is 63 cm. With three outlets the distance can be reduced to 39 cm.

Design decision: *Each puff back pipe will have three outlets over each module. The distance from the outlets to the topmost louver will be 50 cm to ensure that the pulse is fully spread.*

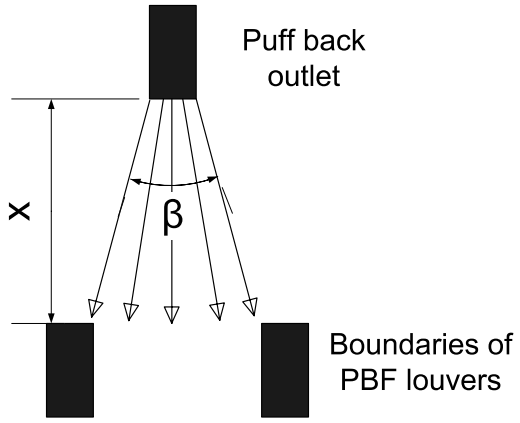

Figure 4.13: Puff back pulse dispersing distance

4.3.5 Sand recycle

At the bottom of the enveloping house, granular medium and dust from puff back regeneration will be collected. Granular medium and dust will be separated, and the granular medium is transported to the filter medium refill system. The separation can be done before or after the transportation process.

Particle dust separation technologies The particles have a median diameter of about 0,7 mm, while fly ash particles from biomass combustion have a diameter of between 10 to 60 μm [4]. The SB particles are approximately ten times bigger than the fly ash. Several separation technologies are applicable.

The gravity settling chamber is the simplest device for separating particles from gas streams. When gas and particles enter the chamber, the gas velocity is reduced. The residence time in the chamber should be long enough so that particles fall out of the gas stream due to the influence of gravity [7]. The chamber can be designed to separate only large particles. A settling chamber is used for separation particles out of a gas stream, thus a gas system is needed.

A cyclone can also be used. The cyclone working principle is described in chapter 4.2. The cyclone can be designed for separating large particles from small fly ash particles in a gas stream. However, using a cyclone will bring about the need for a gas flow system to blow the particles through the cyclone.

Vibrators are used in industrial applications to mix granular mediums, but can also be used to sort different mediums by particle size [2]. The working principle of a vibrator is called the Brazil nut effect: A mixture of particles of different sizes tend to segregate under the influence of vibrations [15]. There are only two variables to adjust; the frequency, f, and the amplitude, a. The vibration intensity

Γ_r is used to classify vibrators:

$$\Gamma_r = \frac{a(2\pi f)^2}{g} \tag{4.6}$$

Segregation occurs when Γ_r is larger than one. Larger particles may segregate to the top or to the bottom of the granular bed, depending on frequency and amplitude [15]. In industrial applications, vibrators are often used in combination with a sieve [2].

A sieve is a perforated surface. The holes are big enough for the dust to fall through, but too small for the granular medium to pass.

Pneumatic transport Several means of particle transport were considered. A comparison of screw feeders, conveyor belts, pneumatic transport and vibrating conveyors is found in Table 4.5. Efficient heat recovery and space efficiency are design conditions. As open systems have greater heat loss, the transport system should be closed. The only acceptable technologies are screw feeders and pneumatic transport systems. Screw feeders are excluded due to experience in a previous project [1]. Although pneumatic transport is more complicated, the technology is found to be the best option for the sand recycle system.

	Screw feeders	Conveyor belts	Pneumatic	Vibration
Size	Compact	Large	Compact	Large
Open/closed	Closed	Open	Closed	Open
Parts	Simple and few	Simple and few	Extensive	Simple and few

Table 4.5: Conveyor technologies comparison

Pneumatic transport systems convey particles by the means of gas transportation [2]. Air is most commonly used, due to availability. Pneumatic transportation systems can be divided into dilute and dense phase transport. In dilute systems particles do not occupy more than 5 % of the volume. Dense transport systems are referred to as plug conveying. The particles can occupy as much as 50 % of the volume, and transport mechanisms are quite complicated due to particle interactions. Transportation mechanisms in dilute phase transport are well understood. The particles are dispersed and dragged by the gas flow, ideally they should be whirled about by turbulent flow [17] [18]. When designing a pneumatic transport

[1] Screw feeders were used in the design of a PBF plant built at Hadeland, Norway for Bjertnes AS. The screw feeders were torn, and the SB could not be used as filtration medium. New screw feeders were supplied, and olivine was used instead. [16]

system, the system can be divided into four subsystems with individual restrictions and limits for the particle transport: [2]

- Particle pick-up
- Horizontal transport
- Vertical transport
- Particle drop-off

The particle pick-up system should be designed without the use of screw feeders and rotary valves, due to the hardness of SB. This leaves venturi feeders, gate lock valves, blow tanks and suction nozzles.

A basic venturi feeder is illustrated in Figure 4.14. At the point were granular medium is fed to the pipe, the cross section is reduced. This causes an increase in air velocity and a decrease in pressure in the throat. The pressure in the throat should be the same as in the supply hopper, so that no air will flow in opposite direction of the material fed. The venturi feeders can only be applied in low pressure systems [7].

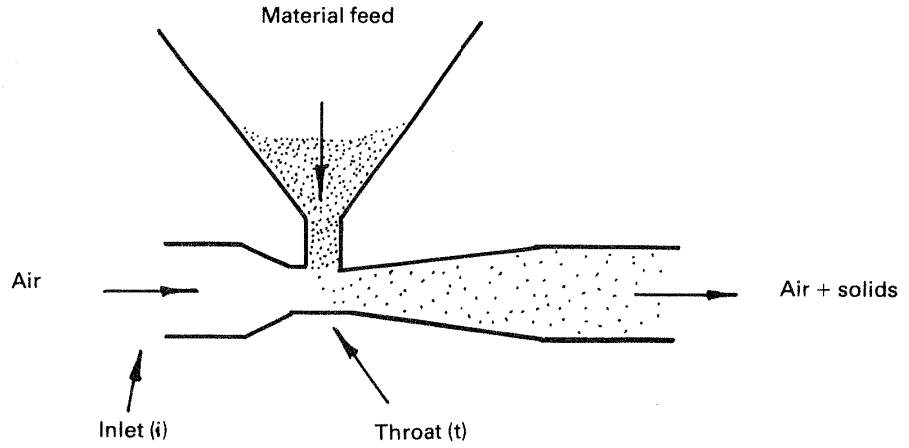

Figure 4.14: Basic venturi feeder [7]

Gate lock valves consist of two gates or doors that are opened and closed to drop material feed from the supply hopper to the conveying line [7], illustrated in Figure 4.15. The conveying line can operate at higher pressures than with venturi feeders due to the hopper being sealed off. For gate lock valves to be applied on SB, the design has to be made so that the supply hopper fully empties. If there is still SB in the hopper, there is a risk that SB can get stuck in the gates. The gates will be torn because of the hardness of SB.

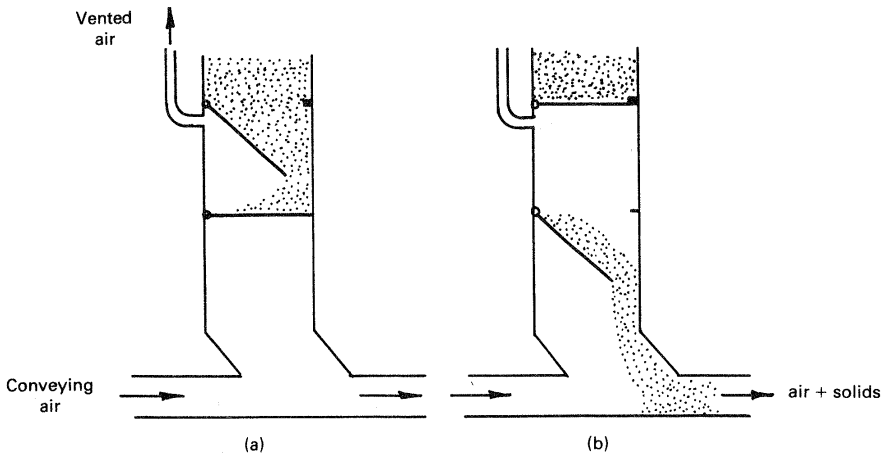

Figure 4.15: Basic gate lock feeding system [7]

A blow tank is illustrated in Figure 4.16. Material is fed from the supply hopper, through an open supply valve. At this time the blow tank is at atmospheric pressure. The supply valve is closed, and air at high pressure is supplied from the bottom, fluidizing the material. The granular material is blown into the conveying line. After the granular material is removed, the blow tank is vented and the cycle starts again. The supply hopper has to fully empty to avoid problems due to the hardness of SB.

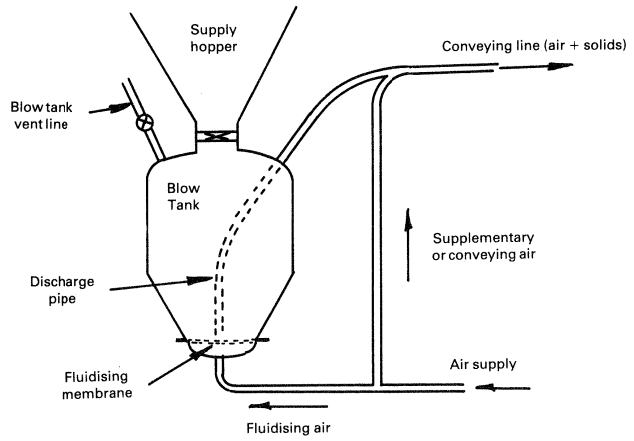

Figure 4.16: Basic blow tank with top discharge[7]

Suction nozzles are used in negative pressure conveying systems. The working principle of suction nozzles is quite similar to domestic vacuum cleaners, although systems for industrial applications are more complex. Sufficient air supply is essential, both at particle pick-up, and once the particles are dragged into the conveying line [7]. Figure 4.17 shows a typical suction nozzle design. At the end of the pipeline, there is a sleeve with the length a. Air supply for material feed is supplied through the space created. The length a has to be sufficient to ensure that the primary air inlet is not buried. The length b in Figure 4.17, is the difference in position of the end of the pipeline and the end of the sleeve. The length b is dependent on the material to be transported, and could be both negative and positive [7]. Secondary air to convey the material is supplied through holes in the pipeline.

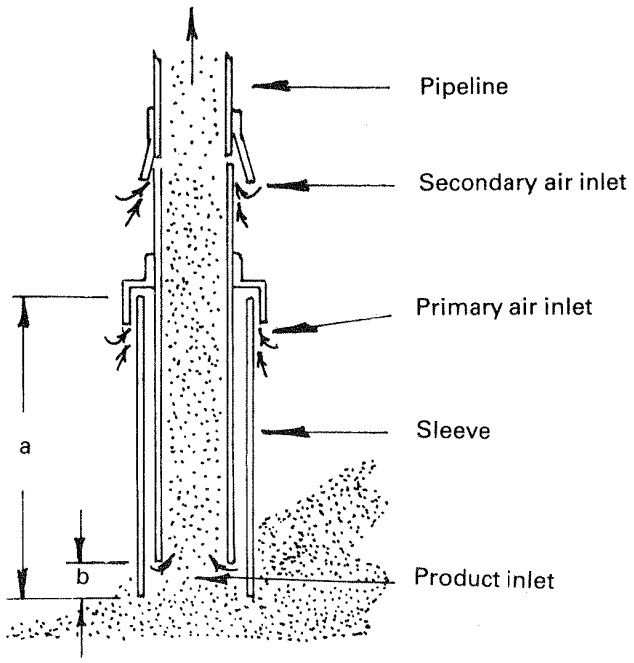

Figure 4.17: Suction nozzle for vacuum pick-up systems[7]

Sand recycle system Two alternative sand recycle systems were considered, and flow charts are supplied in Figure 4.18. Parameters for the pneumatic systems

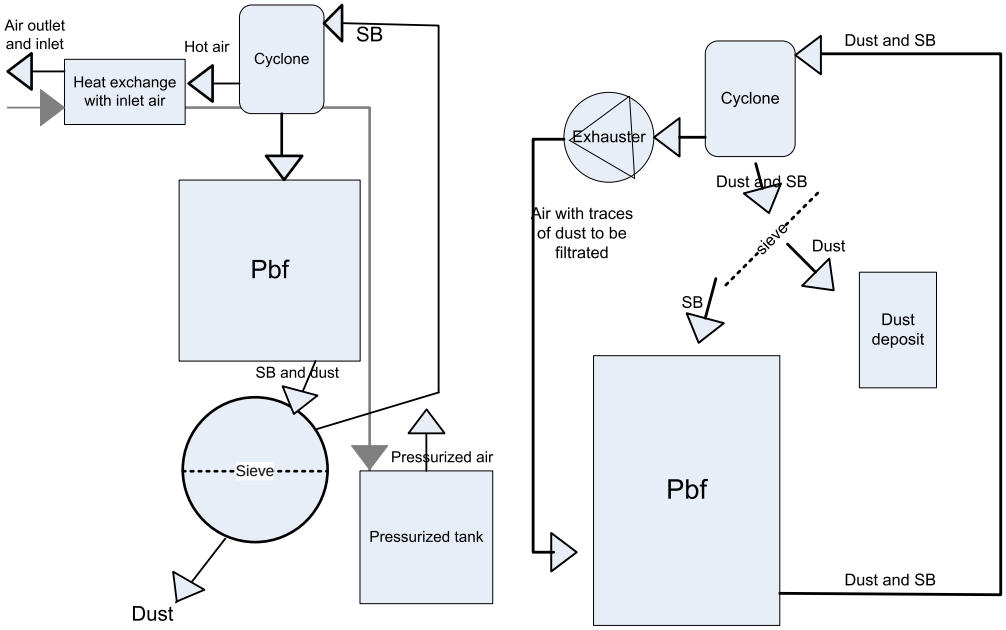

Figure 4.18: Sand refill system design Left: System A, Right: System B

are given in Table 4.6. For system B, both SB and dust will be transported. The dust to SB ratio will be approximately 0,1 kg/kg. The systems will be heated and insulated, so that SB re-entering the filter has a temperature of 450 $°C$.

Sand recycle system A System A resembles the design used in a plant built in Hadeland, Norway. The Hadeland plant was used to clean flue gas from a wood chip combustion plant at Bjertnes Sag AS [8]. Olivin was used in the Hadeland plant. SB will first be separated from the dust in two or three rotating sieves. The dust is deposited, and the SB is then fed to the pneumatic transport system. Blow tanks are used for particle pick-up, and a cyclone will be used for particle drop-off. Pressurized air is supplied from a pressure tank. Air exiting the cyclone is released after heat exchange with inlet air. The blow tanks, the rotating sieves and the piping system can be delivered by Gericke [19]. The cyclone can be designed and built as described in section 4.2.

Sand recycle system B System B is illustrated on the right in Figure 4.18. The sand and SB is sucked up from the bin in a vacuum pneumatic conveying system. The suction nozzles used for particle pick-up can be supplied by PIAB [20]. The suction nozzles should be able to move up and down in the bins, to keep the suction nozzle from being buried. Sensors on the nozzle are required to controll the nozzle position. The inside of the pipes will be covered with ceramic material to avoid wear and tear due to the hardness of SB. Most of the particles and dust are separated from the air in a cyclone. Dust is then separated from the SB in a sieve. The SB is fed to the PBF. An exhauster is sucking air through the pneumatic system and the cyclone. The exiting air is fed to the PBF to be cleaned.

Material	Sintered Bauxitt 20/40
Terminal gas velocity	5,89 m/s [2]
Mass flow, U_s=0,1 m/s	min: 16,5 g/s max: 44,0 g/s
Mass flow, U_s=0,2 m/s	min: 22,9 g/s max: 61,1 g/s
Temperature range	from 400 $°C$ to 450 $°C$
Vertical pipe length	ca. 4 m
Horizontal length	ca 2 m
Number of bends	2 (90 °)

Table 4.6: Parameters for the pneumatic system

The particle supply of sand recycle system B is simple, as the particles are sucked directly into the pipe through the suction nozzle. The system can easily be designed without any screw feeders or gate lock valves. For sand recycle system A, some sort of equipment for controlling the amount of SB particles supplied to the blow tank must be installed.

Design decision: *Sand recycle system B is chosen. The system, consisting of suction nozzles, a cyclone, a sieve and a fan, is shown in Figure 4.18.*

SB distribution system The SB from the sand recycle system is supplied to the SB distribution system on the center of the rooph of the enveloping house. A screw feeder, as illustrated in Figures 4.19 and fig:sbdistribution, will be used to distribute the SB in the direction of the module columns. The distance between the screw feeder and the wall will be large, to ensure that SB particles are not trapped. The screw will move SB particles along the module rows. The SB is distributed between the module rows trough pipes with angles above the angle of repose for SB. The distribution through the pipes is assisted by gravity. The piping system illustrated in Figure 4.20 will be built.

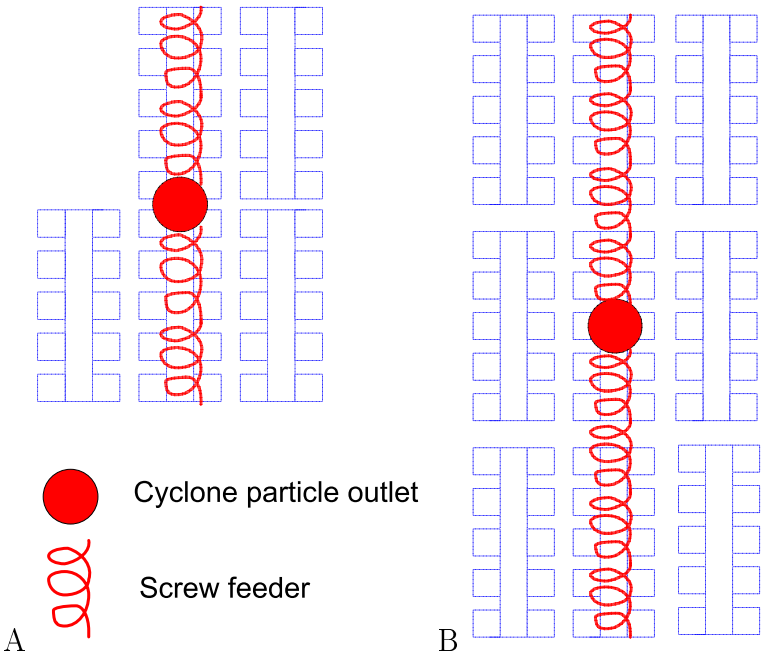

Figure 4.19: SB distribution with a screw feeder A: U=0,2 m/s, B: U=0,1 m/s

Design decision: *SB will be distributed between the module columns using a screw and pipes with angles exceeding the angle of repose for SB. The distribution system is illustrated in Figures 4.19 and 4.20.*

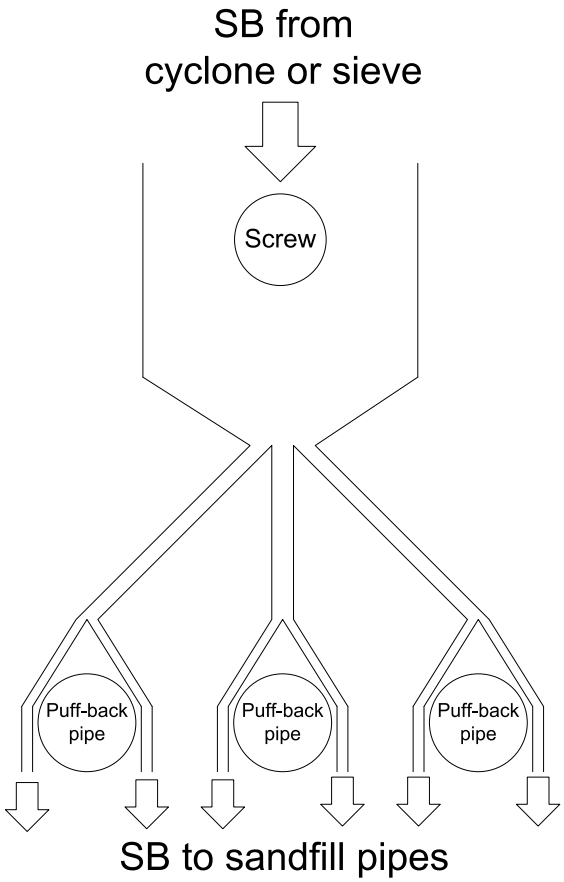

Figure 4.20: SB distribution piping

4.4 Summary of the PBF system design

Flue gas enters the filter system with a dust concentration of 450 mg/Nm^3. Approximately 95 % of the particles are removed in a cyclone before the gas enters the PBF.

The PBF has filter tray louvers similar to those described in chapter 3. The louvers will be wider (0,5 m), and the vertical distance between the louvers will be reduced. The area ratio is set to 1,7. The PBF modules are double-sided with 46 louvers on top of each other on either side. The modules are arranged in module columns with five modules next to each other. The modules in each module column share the same clean air duct and the same puff back system. The number of module columns, the module column area and the area required for the enveloping house is given in Table 4.7.

A puff back pipe with three outlets is placed 50 cm above each module column,

parallel to the clean air duct. The puff back pipes are connected to a high pressure reservoir through a high speed valve. When the modules are cleaned, the clean gas flow is stopped, and a pressure pulse is released into the puff back pipe. The pressure pulse spreads out through the outlets, and SB and dust cake fall off the louvers when the pulse hits. Puff back cleaning is initiated when the pressure drop over the entire filter reaches a set value. All the module columns will then be cleaned in a set sequence with a set time delay. The time delay, the sequence and the pressure drop should be found through calibration tests. The sandspill is collected in bins at the bottom of the enveloping house. The number of bins is given in Table 4.7.

Design variable	U_s=0,1 m/s	U_s=0,2 m/s
Number of module columns	9	5
Module column area	28,71 m^2	18,4 m^2
Enveloping house area	17,29 m^2	11,53 m^2
Bins at the bottom of the enveloping house	3	2

Table 4.7: Summary of the PBF system design

A vacuum pneumatic conveying system will bring dust and SB to the top of the filter. There will be one suction nozzle in each bin, and one fan will suck the SB and dust through the pipes. A cyclone will separate the particles from the gas flow. The gas exiting the cyclone will be cleaned in the PBF. The dust is separated from the SB in a sieve. The SB is spread out to all the modules using one screw feeder, and pipes with angles above the angle of repose for SB.

The whole system will be heated and insulated to keep flue gas temperature as high as possible.

Chapter 5

Experimental tests with BioSOFC filter

5.1 Introduction

Heating experiments were conducted on the BioSOFC filter before the whole filter system with fans and a heat exchanger was shipped to Güssing in Austria for field testing at a biomass gasification plant. The objectives of the heating experiments were to find a good heating procedure, and to test if the heat supplied was sufficient to avoid any risk of tar condensation. Producer gas must be filtrated at 500 °C. Tar may condense if the temperature falls below this limit. Condensed tar is very sticky, and will cause harm to the fans and other moving, mechanical equipment. Puff back tests were also performed to demonstrate the repeatability of the puff back calibration tests from earlier work [21]. The heating experiments and puff back tests are presented in this chapter.

5.2 Description of the filter module

Figure 5.1 shows the filter module designed for the BioSOFC process. The module is two-sided, with 55 louvers on either side. SB is used as filtration medium. The filter was dimensioned for a volume flow of 20 Nm^3/h. Only half the capacity will be used during field testing. The filter is placed in an enveloping house. Exact measures are found in Figure 5.2. The enveloping house has one gas inlet, two gas outlets through the PBF and one sand and dust outlet in the bottom.

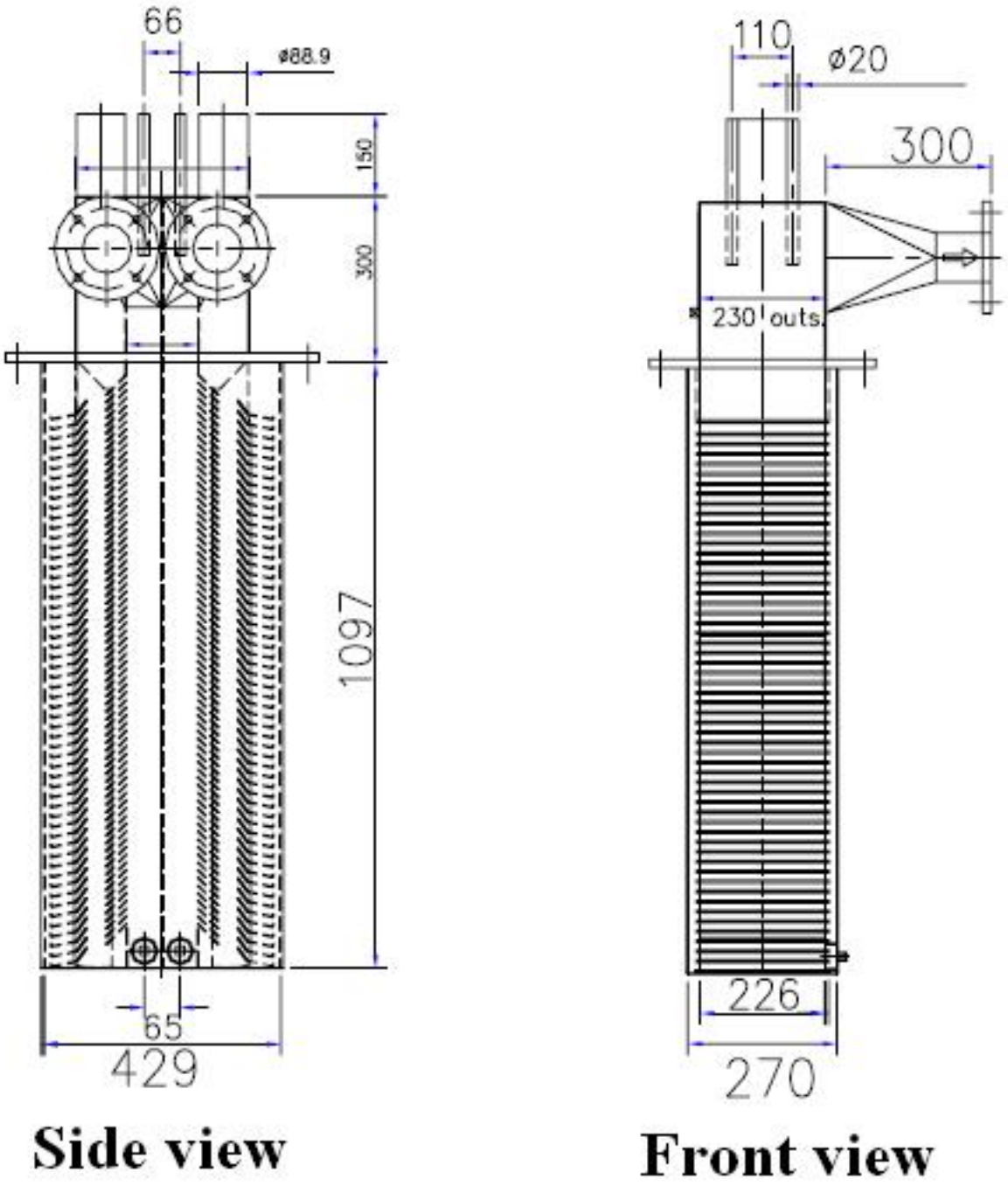

Figure 5.1: The BioSOFC filter unit

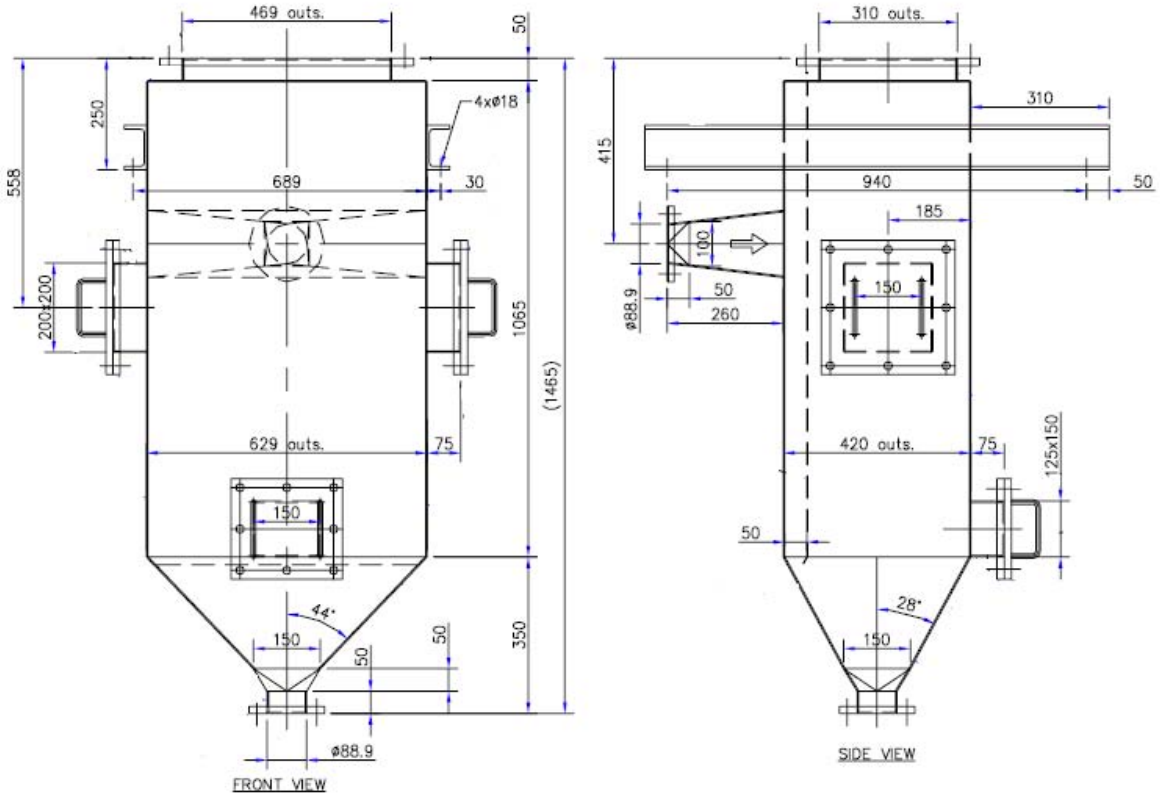

Figure 5.2: The BioSOFC filter enveloping house

The parts of the filter system are illustrated in Figure 5.3. As the filter is two-sided, there are two puff-back pipes, two sandfill pipes, two boxes and two manual valves. The gas stream is split in the PBF and merged before the H_2S removal unit.

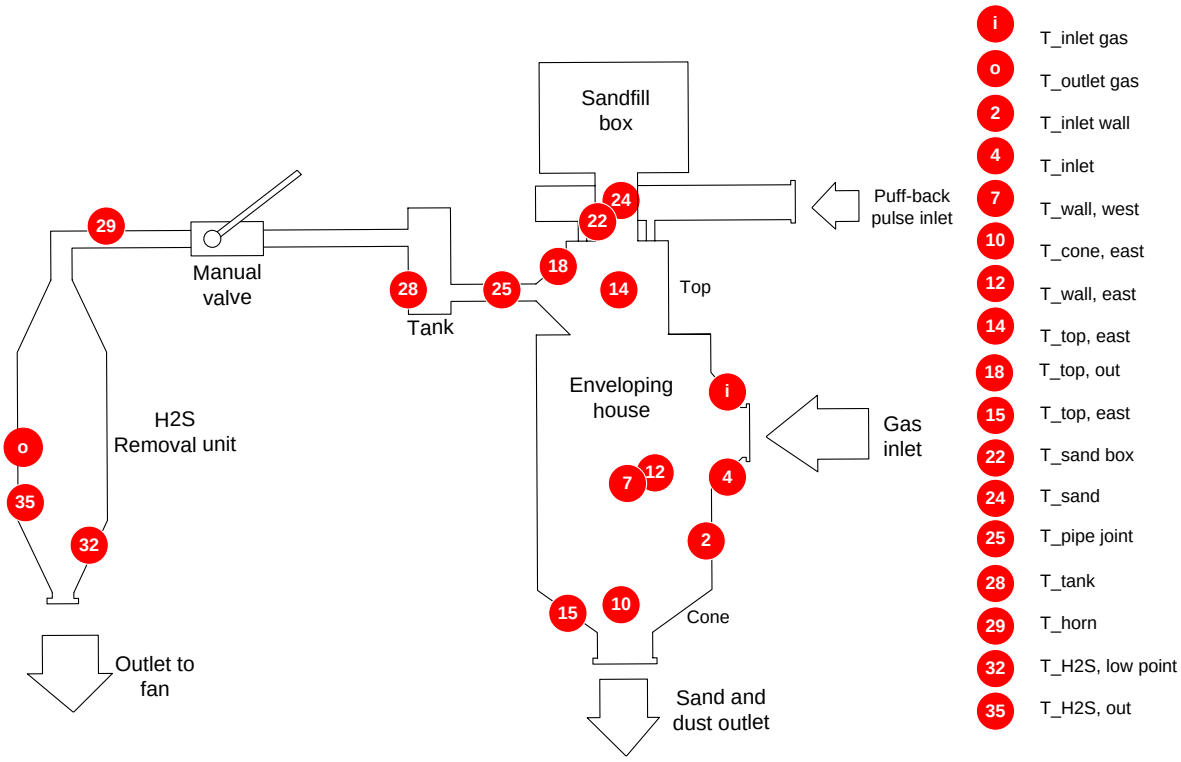

Figure 5.3: The BioSOFC filter system and the placements of thermo couples for the heating tests

5.2.1 Heating cables

The enveloping house has been dressed with Kanthal D heating cables and insulation. Each heating cable is covered with a ceramic material. Kanthal D heating cables can endure temperatures up to 1350 °C, and have an ohmic resistance of 0,35 Ω/m. The heating power is given by equation 5.1.

$$P = \frac{V^2}{R_\Omega} \tag{5.1}$$

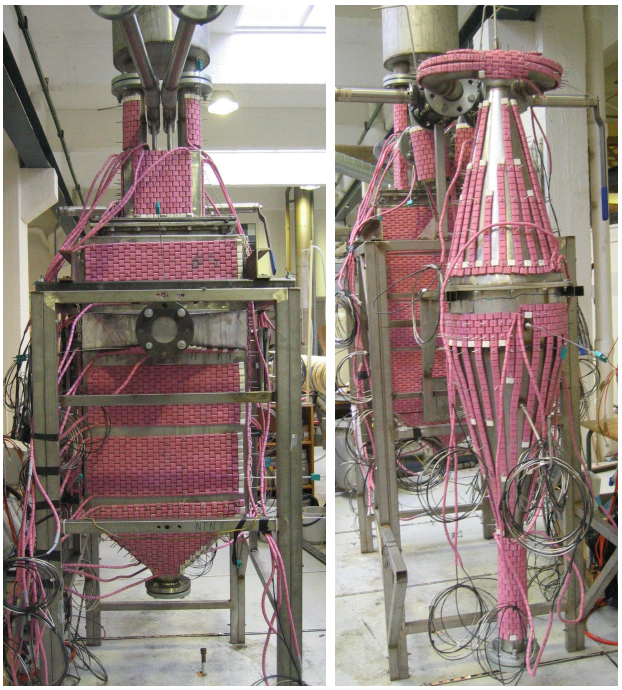

Figure 5.4: BioSOFC filter with heating cables

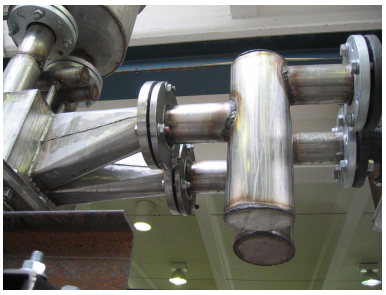

Figure 5.5: The pipe joint and the tanks

P is the heating power, V is the voltage and R_Ω is the ohmic resistance. The heating is regulated by a PID (proportional-integral-derivative)-controller, set to the desired temperature. The controller is supplied with temperature measurements. The PID-controller feeds the heating cables with a voltage a certain part (A) of the time, depending on the measurements. The output power P_{output} is given by equation 5.2.

$$P_{output} = A * P_{maximum} \tag{5.2}$$

$P_{maximum}$ is the maximum heating power. The heating cables produce maximum power when supplied with a voltage. A maximum value for the time percentage A is set. During continuous operation, A will be balanced (A_b), and heat from heating cables equals the heat loss.

35 heating cables are mounted on the PBF system as illustrated in Figure 5.4. They were connected in three heating cable circuits. The partitions are given on the CD at the end of the thesis. One temperature measurement input must be supplied to the PID controller for each circuit. Specifications for the heating cables are given in Appendix C.

5.2.2 Thermocouples

The temperature was monitored at 16 points using thermocouples (type K). Two measuring points are in the gas stream, while the rest have numbers corresponding to the placements of the heating cables. The placement of the thermocouples are given in Figure 5.3.

5.2.3 Insulation

All the components are covered with five layers of insulation. There are two layers of superwool, and three of rockwool. The outer layer is covered with aluminum foil. Specifications for rockwool and superwool are given in Appendix C. The insulation thickness for the layers are given in Table 5.1.

Layer	Type	Thickness
1	Superwool	2,5 cm
2	Superwool	2,5 cm
3	Rockwool	8 cm
4	Rockwool	8 cm
5	Rockwool with aluminum foil	2,5 cm

Table 5.1: Insulation layers

5.2.4 Logging system

The computer logging system was made by Daniel Stanghelle in LabVIEW. Temperatures from the 16 measuring points were logged every second.

5.3 Heating experiments

The main objective of the heating experiments was finding PID input values that would optimize operation in Güssing. The optimization included finding the thermocouples most suited as temperature input for the PID-controller, and to heat the entire PBF system to 500 °C in a rapid and controlled manner. Good measuring points should be a representative of the other temperature points in the same circuit. Another objective was to test if the heating and insulation mounted was adequate to keep the whole filter system at a temperature above 500 °C.

5.3.1 Experiment, set up and procedure

The filter system was mounted and filled with SB. The experiments were conducted without gas flow, and with no dust in the filter.

Three heating experiments were conducted. During the first two experiments, the filter system was only heated to approximately 250 °C. The goal of the first two tests was to find good temperature measuring points to use as input to the PID-controller. The heating cable circuits were monitored to see that the filter was heated approximately evenly. After setting the temperature inputs for the PID-controller, the filter was heated to 500 °C. The goal of this last experiment was to find good settings for the PID-controller. The PID time interval, t' was 2 seconds, for all the experiments.

5.3.2 Results

First heating experiment Figure 5.6 show the temperatures at the 16 measuring points during the first heating. The PID control value A, was set to a low value. The PBF was heated slowly to avoid possible damage on heating cables caused by rapid heating. The temperature measuring points used as input for the PID controller during the first experiment are given in Table 5.2. After three hours, the temperature input for circuit 2 was changed. The temperature of thermocouple T_top,out (18) was high compared to the other temperature measuring points, as shown in figure 5.6. Thermocouple T_wall,east (12) was used instead. The change of the thermocouples are shown in figure 5.6.

Circuit	Termocouple
Circuit 1	T_wall,west (7)
Circuit 2	T_top,out (18)/T_wall,east (12)
Circuit 3	T_horn (29)

Table 5.2: Temperature inputs for the PID controller, first experiment

The PID-control values (A maximum) for the three circuits are given in Table 5.3. The balanced A values, A_b, for the first heating experiment were not recorded due to human error.

	Temperature input	t=0 h	t=1 h	t=1,8 h	t=3 h	t=3,2 h
Circuit 1	Wall, west (7)	10%	15%	20%	25%	30%
Circuit 2	Wall, east (12)	10%	15%	20%	25%	30%
Circuit 3	Horn (29)	10%	15%	20%	25%	30%

Table 5.3: PID-controller values (Maximum A), 080607

The temperature distribution after the first heating is illustrated in Figure 5.7. The difference between the highest and the lowest temperatures was about 150 °C. The temperature was low in the sand, the pipe joint and in the H_2S unit. Thermocouple 28, measuring the temperature of the tank, was not functional.

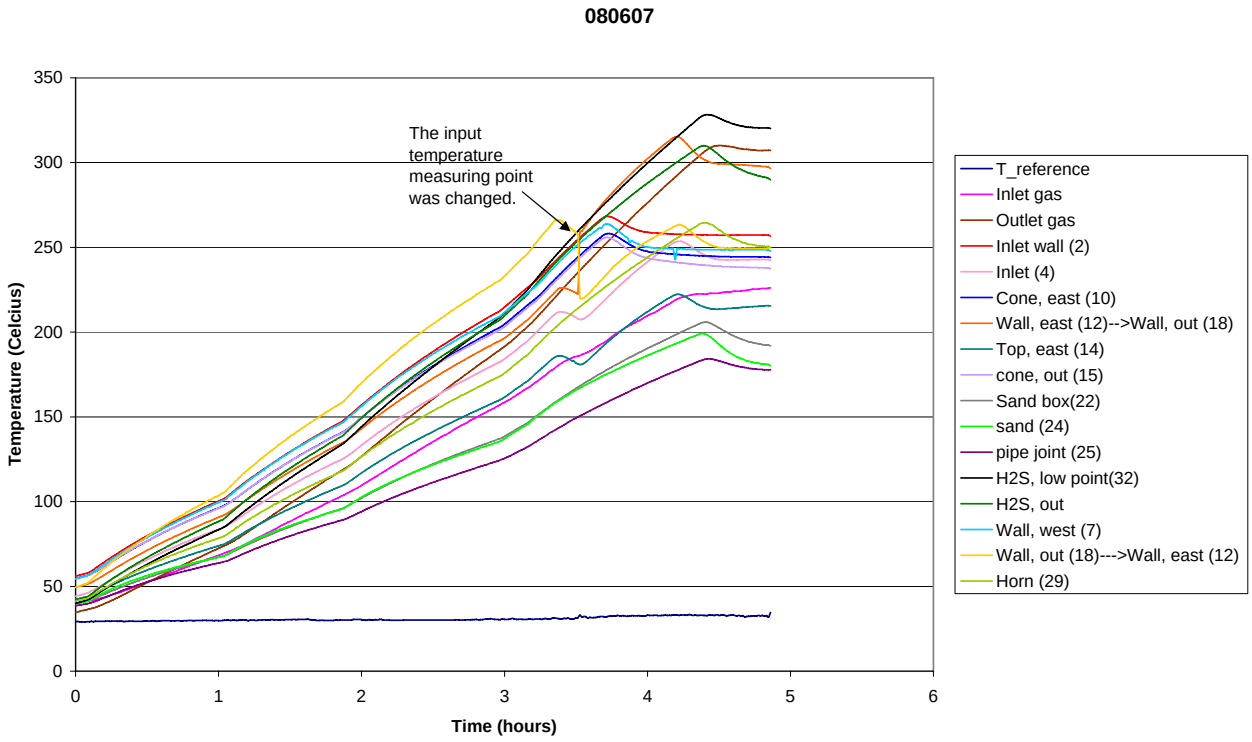

Figure 5.6: Temperatures during the first heating experiment (080607)

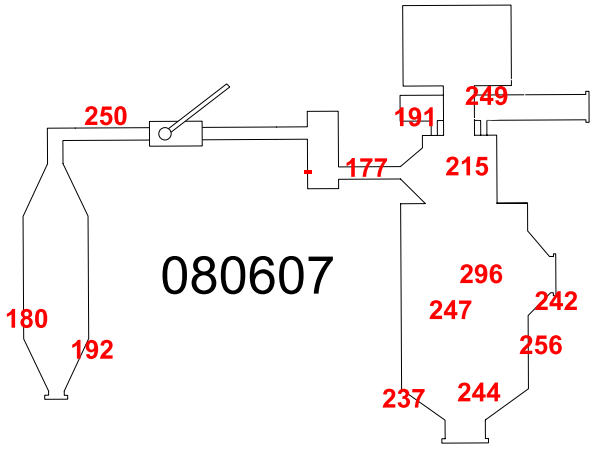

Figure 5.7: Temperature distribution after the first heating experiment (080607

Second heating experiment The heating cable circuits were modified to improve the results after the first heating experiment. The modifications were made by Daniel Stanghelle, and circuit partitions are found on the CD at the end of the thesis. The temperature measuring points used as input for the PID controller found during the second part of the first experiment were used. The input measuring points are given in Table 5.4. Figure 5.8 shows the temperature during the

Circuit	Termocouple
Circuit 1	T_wall,west (7)
Circuit 2	T_wall,east (12) *)
Circuit 3	T_horn (29)

Table 5.4: Temperature inputs for the PID controller

second heating experiment and during the cooling afterwords. The PID-control inputs, A, were increased, resulting in an increased temperature growth. The temperatures were more even than after the first heating, but there were still a temperature range between the highest and the lowest temperatures of about 100 °C. The temperatures of the H_2S unit and the tank were still low. The balanced values for the PID control input A_b, are given in Table 5.5. After the heating was turned off, the temperature was logged through the night.

	Temperature input	A	A_b
Circuit 1	Wall, west (7)	15 %	8-9 %
Circuit 2	Wall, east (12)	25 %	9 %
Circuit 3	Horn (29)	25%	10-11 %

Table 5.5: PID-controller values, 090607

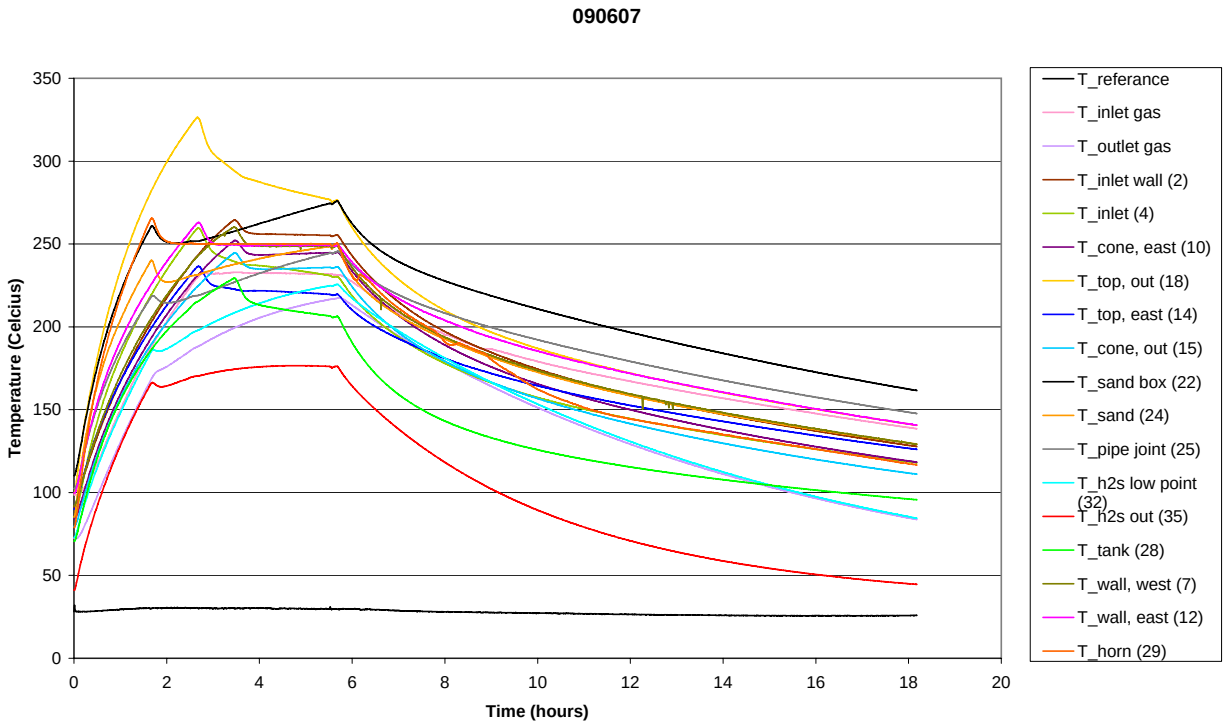

Figure 5.8: Temperatures during second heating experiment (090607)

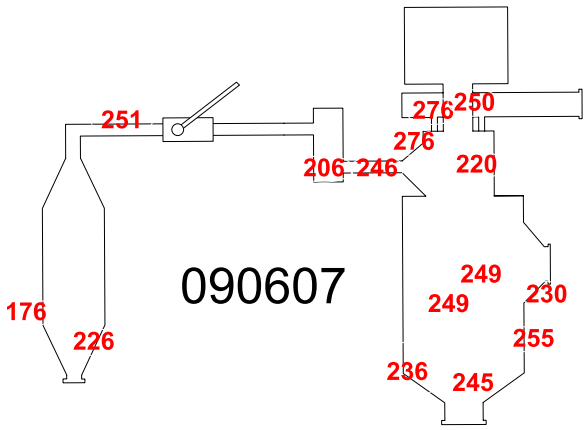

Figure 5.9: Temperatures after second heating experiment (090607)

Third heating experiment Figure 5.10 shows the third heating experiment. The PBF was heated to about 500 °C. Temperature measurement inputs for the PID controller were the same as in the second experiment (Table 5.4). During the first hour of the heating process, the input values (A) used during the second experiment were used. The values for A were then increased and balanced as given in Table 5.6. Figure 5.11 illustrates the temperature distribution after the heating experiment. The temperatures were still low in the tank and in the H_2S unit, and very high in the sandbox. The temperature range was about 250 °C.

	Temperature input	t=0 h	t=0,9 h	t=1,8 h	A_b (t=12 h
Circuit 1	Wall, west (7)	15%	25%	35%	17-18%
Circuit 2	Wall, east (12)	25%	25%	35%	15-16%
Circuit 3	Horn (29)	25%	25%	35%	28-29%

Table 5.6: PID-controller values , 100607

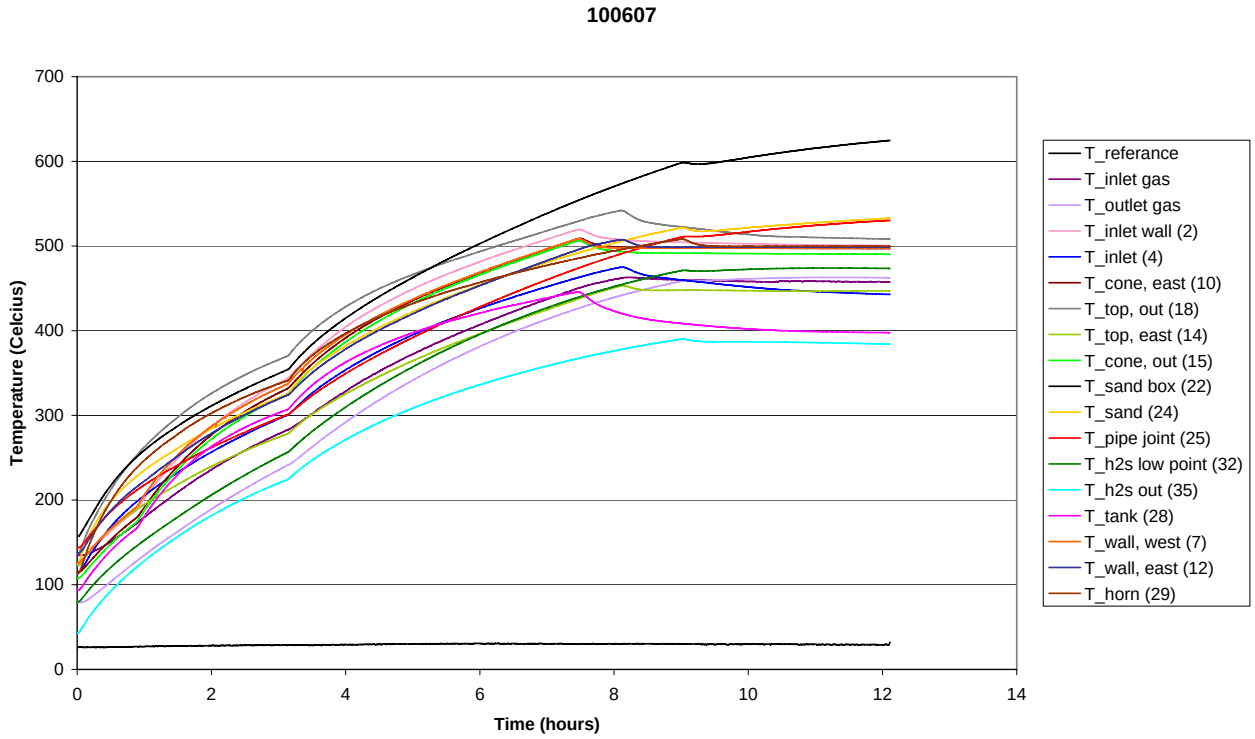

Figure 5.10: The temperature course during third heating experiment (100607)

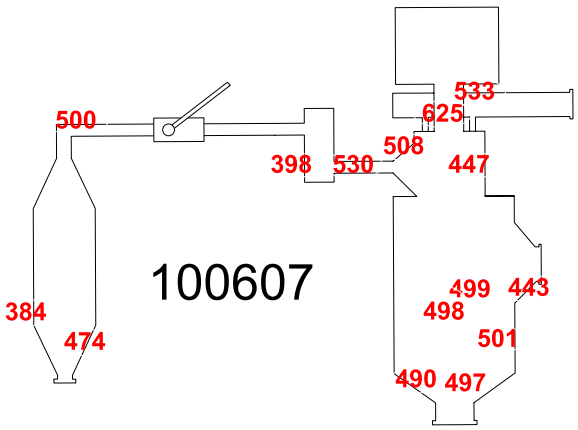

Figure 5.11: Temperature distribution after third heating experiment (100607)

5.3.3 Comments on the heating experiments

Temperature measuring point inputs for the PID controller were found during the first heating experiment, and are given in Table 5.4. The temperatures of three inputs were around the mean value for the filter temperature, and are believed to be suitable.

The temperature difference during the third heating experiment was almost 250 °C as shown in Figure 5.9. A temperature range of about 50 to 60 °C would be acceptable if most temperatures were above 500 °C. The temperature problem zones are given in Table 5.7. The areas with the lowest temperatures are found in

Low temperatures	The H_2S unit, the tanks and the pipe joint
Moderately low temperatures	The top box and the gas inlet
High temperatures	The sand box

Table 5.7: Temperature problem zones for the BioSOFC filter

the H_2S unit, and in the tank. During the first experiments the temperature was low in the pipe joint and the sand. The temperatures were moderately low in filter inlet and the top box. The temperature in the sand was very high during the last experiment. All heating experiments were performed without gas flow through the system. A hot gas flow will even out the temperatures in the system, but with wall temperatures as low as 384 °C, gas cooling and tar condensing may be cause problems.

The cooling of the filter system shown in Figure 5.8 show that three of the thermocouples (T_h2s out (35), T_h2s low point (32) and T_outlet gas) record

a more rapid temperature fall than the average. The three thermocouples were all placed on the H_2S unit. During all heating experiments, these areas were difficult to heat. The temperature fall suggests that the difficulties were caused by high heat losses: The H_2S unit outlet was closed with a metal plate without any insulation, and heat convection with surrounding air may have caused the heat loss.

The outlet will be connected to heated pipes during field testing. This will reduce the heat loss, but there is a risk that temperatures will still be low. There may be insufficient insulation or low heating cable effect contributing to the disappointing results.

The gas inlet to the filter was also covered with a metal plate without any insulation. Heat convection from the metal plate may have been the reason the inlet area (the top box and gas inlet) had moderately low temperatures. Figure 5.6 did not show a great heat loss, as for the H_2S unit. Unlike the H_2S unit, the inlet and the top box are surrounded by other hot parts. Heat conduction from other parts of the filter may have kept temperature high. This may why temperatures in the gas inlet area were not as low as in the H_2S unit.

During the first experiment the sand box did not reach a high temperature, while the sand box was the warmest part of the system during the third experiment. The slow heating was due to the great mass of the sand. The sand box receives heat from the hot filter below, as heat rises. Some insulation should be removed to make sure the temperature does not increase uncontrolled.

The tanks and the pipe joint seemed to be difficult to heat. The difficulty is believed to be caused by the geometry because covering the pipe joint and the tanks with heating cables was difficult. The pipe joint had a good heating curve during the last experiment. The change may have been caused by the hot sand box in the near vicinity of the pipe joint. Insulation will be removed from the sand box, and the temperature in the pipe joint will probably fall. The heat loss from the pipe joint and the tanks (shown in Figure 5.8) seem to be acceptable. The low temperatures are not caused by insufficient insulation. There are two measures to improve the heating performance:

- The heating cable circuits can be modified to increase power supplied through the heating cables covering the tank and the pipe joint. The power supplied to the filter inlet area and the top box should also be increased.

- The cabling can be re-done covering a larger part of the pipe joint and the tanks.

Modifications of the circuits are simpler than changing the heating cables. This work proposes that modifications to the heating cable circuits should be made,

and that new experiments should be performed with gas flow through the system before the field testing.

5.4 Puff back tests

Calibration tests of the puff back pulse for the BioSOFC filter has been presented in earlier work [21]. In this work the calibrations were done before the filter was mounted in the enveloping house. The best sandspill results from the calibration tests was releasing the puff back pulse from an 8,5 liter tank with pressurized air at 3,5 bar. Ideal sandspill calculated to be 44 g from each louver, or 2,42 kg from either side of the filter.

Puff back tests were in this work performed to demonstrate that the filter was operational. Puff back tanks were mounted, and filled with pressurized air from the laboratory grid. Puff back pulses were released and the sandspills were collected and measured.

5.4.1 Results

Results from puff back tests are give in Tables 5.8 and 5.9. Puff back tests for three pressures were performed for each side of the filter, because the sandspill differed from the sandspill found during calibration experiments,

Experiment	Pressure in tank (bar)	Sandspill (kg)
1	3,5	4,995
2	3,5	5,167
3	3,5	5,586
4	3,5	5,241
5	3,1	3,306
6	3,1	3,722
7	3,1	3,887
8	3,1	4,192
9	2,5	2,055
10	2,5	1,986
11	2,5	1,862
12	2,5	1,953

Table 5.8: Puff back sandspill from the east side of the BioSOFC filter

Experiment	Pressure in the tank (bar)	Sandspill (kg)
1	4	2,010
2	4	2,391
3	4	2,529
4	4	2,578
5	3,5	1,239
6	3,5	1,267
7	2,75	0,286
8	2,75	0,317

Table 5.9: Puff back sandspill from the west side of the BioSOFC filter

5.4.2 Comments to puff back tests

The sandspills were not even on the two sides, and differed from results found during the calibration tests [21]. Therefore puff back tests were performed with pressures above and below calibration value (3,5 bar) [21]. The sandspill from the West side was too low, while the sandspill from the East side was too high. The reason for the difference in sandspill was that the filter was not leveled. The misalignment was never measured, but the sandspill suggests that the filter was leaning to the East. New tests could not be performed as the filter was due to be shipped to Austria. The filter will be leveled when mounted in Güssing, and the sandspills should be adequate on both sides.

Chapter 6

Conclusions and recommendations for further work

6.1 The filter tray louver

A filter tray PBF has been successfully designed and built. Only limited testing has been performed on the unit due to lack of time. Puff back tests have been performed, and have shown that the louvers can be cleaned by puff back. The best louver for SB had an angle of 22 °. The bed was even, and the sandspill was good. The activation pressure for the filter tray louvers were low (3,25 to 3,9 mbar). Louvers with an angle of 22 ° or below were stable, and no SB would spill from the louver between puff backs.

Further work The further work with the filter tray louvers are divided into two categories (although the two are intertwined): Improvements to the filter tray design and further experimentation.

Improvements to the filter tray design:

- Find the maximum length of the louver. Longer louvers give larger filtration surface area. However, sandspills from very long louvers will not be even. The ideal louver length should be found through puff back experiments.
- Decrease the height between the louvers. The height between the louvers was over-dimensioned. The clean gas volume of the next louver above should be directly above the sandfill holes.
- Experiment with v-shaped slide plates. The v-shaped slide plate will increase filtration surface.

- Variations in the clean gas volume. With a lower clean gas volume, the nominal face area is reduced and the area ratio Θ is increased. The clean gas volume and the shape of the volume determine the spills from the louver during puff back cleaning as the flow of the puff back gas is affected. Different geometries should be investigated, and the most space efficient design with the best sandspills should be used.

Further experimentation :

- Investigate the sandspill using a high speed camera. The mechanisms of the sandspill should be investigated to see that the granular medium spills from the whole louver area.

- Filtration tests should be performed to see that the shallow beds efficiently remove dust from gas, and to prove that the filter tray technology is fully functional.

- The design of filter tray PBFs for other granular mediums should be made.

6.2 The industrial PBF system design

A PBF system for filtrating the flue gas from a hypothetical biomass combustion plant has been designed. The heat in the flue gas is to be used for district heating after the filtration. The PBF system design includes a cyclone, PBF modules with filter tray louvers, a sand recycle system, a puff back system and a sieve.

Further work

- The pressure loss through the system should be calculated, and fans should be designed.

- An estimation of the heat losses should be made, to calculate the need for heating cables and insulation.

- The heat recovery should be estimated and compared to the heat loss. Efficiency for the entire system should be estimated.

- A present value calculation of the plant should be made.

6.3 The BioSOFC project

The BioSOFC filter system was heated to about 500 °C, but the temperatures were not even. The temperature difference between the hot and the cool parts of the system was about 250 °C. The lowest temperatures measured were below 400 °C, which is unacceptable. The temperature was too hot in the sandbox, and low in the H_2S unit, the pipe joint and the tanks. The high temperature in the sandbox can be reduced be removing some insulation. The low temperature in the H_2S unit was caused by the lack of insulation over the gas outlet. During operation, the outlet will be connected to hot pipes, and the temperature loss will be reduced. The low temperature of the pipe joint and the tanks were caused by insufficient heating effect. This work proposes that modification of the heating cables or the heating cable circuits should be made.

Puff back tests on the two sides of the filter were also performed. The sandspills were uneven because the filter had not been leveled. The filter will be leveled in during field testing, and the sandspills are believed to be improved.

Further work This work proposes that the heating cable circuits should be modified to achieve an even temperature distribution. New heating experiments should be performed on-site before field testing. Puff back tests should be performed when the filter is leveled.

Bibliography

[1] Lee, Rodon, Wu, Pfeffer, and Squires. The panel bed filter, epri af-560. final report EPRI AF-560, The city college og the city university of New York, 1977. Research project 257-2.

[2] Daniel Stanghelle. Gassrensing med granulært filter for høytemperatur anvendelser. Master's thesis, NTNU, 2004.

[3] Lecture notes from subject TEP4212: Environmental and cleaning technologies, fall 2006.

[4] Håvar Risnes. *High temperature filtration in biomass combustion and gasification processes*. PhD thesis, NTNU, 2002.

[5] A. M. Squires. Granular-bed filtration assisted by filter-cake formation: 4. advanced design for panel-bed filtration and gas treating. *Powder Technology*, 155:74–84, 2005.

[6] Germot Krammer. Lecture notes from the subject Environmental and cleaning technologies TEP4212, fall 2006.

[7] David Mills. *Pneumatic conveying design guide*. Butterworths, 1990. ISBN 0-408-04719-4.

[8] Magnus Paulsen. Gassrensing med granulært filter. Master's thesis, NTNU, 2006.

[9] Victor L. Streeter. *Handbook of fluid dynamics*. McGraw-Hill Book Company, inc, 1961. ISBN 07-0-62178-0.

[10] A.M. Squires. United state patent, no 7,033,556, april 2006.

[11] Conversation with Otto Sønju 29.4.2007.

[12] Sjaak van Loo and Jaap Kopperjan (Editors). *Combustion and Co-Firing Biomass, handbook*. Twente Univerity Press, 2002. ISBN 9036517737.

[13] Øivin Saanum. Videreutvikling av panelbedfilter for rensing av høytemperatur røykgass. Master's thesis, NTH, 1996.

[14] Magnus Paulsen. Gassrensing med granulært filter. Technical report, NTNU, 2005. Prosjektoppgave.

[15] J. Ellenberger, C. O. Vandu, and R. Krishna. Vibration-induced granular segregation in a pseudo-2d column: The (reverse) brazil nut effect. *Powder Technology*, 164:168–173, 2006.

[16] Conversation with Daniel Stanghelle.

[17] Martin Straub, Sean McNamara, Hans J. Herrmann, Gerhard Niederreiter, and Karl Sommer. Plug conveying in a vertical tube. *Powder Technology*, 162:16–26, 2004.

[18] Katharine Albion, Lauren Briens, Cedric Briens, and Franco Berruti. Flow regime determination in horizontacl pneumatic transport of fine powders using non-intrusive acoustic probes. *Powder Technology*, 172:157–166, 2006.

[19] Internet page: www.gericke.net.

[20] Internet page: www.piab.com.

[21] Ingunn Natvig. Gassrensing med granulært filter for høytemperatur anvendelser. Technical report, NTNU, 2006. Prosjektoppgave.

Appendix A

Characteristics of granular mediums of interest

Saint-Gobain Proppants 20/40 Sintered Bauxite

Typical Properties

Size and Shape Sieve No.	% Retained
20	5
30	75
40	20
<40	TR

TR = Trace

Median Particle Diameter = 0.662 mm
= 0.026 inches

Shape/Sphericity (Krumbein & Sloss) 0.9

Physical Properties		
Bulk Density	2.04 g/cc 127 lbs/ft^3	
Specific Gravity	3.5 g/cc	
Absolute Volume	0.0347 gal/lb	
Acid Solubility, %	1.9	
Crush Resistance @ Stress %	7,500 psi 10,000 psi 12,500 psi 15,000 psi	0.5 1.2 2.2 4.0

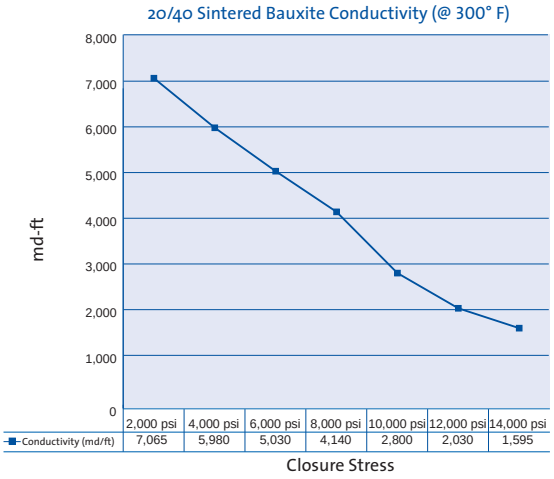

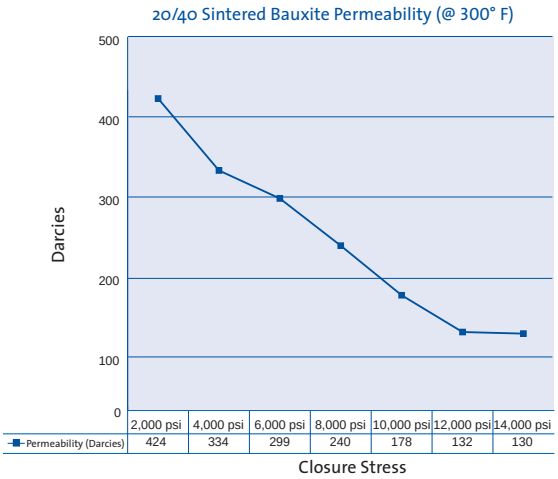

C.D.S. CONSULTANTS
Surface finishing equipment consultants
BWLCH TOCYN FARMHOUSE
BWLCH TOCYN
ABERSOCH
PWLLHELI
GWYNEDD LL53 7BN
EMAIL:Cdsconsultants@btinternet.com
TEL 01758 71 2245
FAX 01758 712014

OLIVINE EXPENDABLE ABRASIVE DATA SHEET

PRODUCT- OLIVINE EXPENDABLE ABRASIVE

DESCRIPTION

A natural mineral blasting abrasive mined from a single large ore deposit. It is essentially a magnesium-iron silicate and contains no free silica.

CHEMICAL ANALYSIS

ELEMENT	%
SILICA $Si0_2$	41 - 43
Magnesium as MgO	47.5 - 50
Iron as Fe_2O_3	6 - 8
Aluminium as Al_2O_3	0.4 - 0.5
Nickel as NiO	0.3 - 0.35
Chromium as Cr_2O_3	0.2 - 0.3
Manganese as MnO	0.05 - 0.1
Calcium as Ca0	0.05 - 0.1
Free Silica	< 1

WATER SOLUBLE SALTS

Conductivity of aqueous extract	< 15 mS m^{-1}
Chloride	< 10 ppm

MECHANICAL ANALYSIS

Hardness	7-8 Mohs
Apparent density	3.3 kg dm^{-3}
Bulk density	1.7-1.9 kg dm^{-3}
Grain shape	Angular
Colour	Pale green

GRADES AVAILABLE

GRADE	SIZE RANGE (MM)
ADD20/FG	0.355 - 2.36
AFS30	0.18 - 1.00
ADD50/FG50	0.125 - 0.50
AFS80	0.09 - 0.25

ABRASIVE PERFORMANCE

Appendix B

Slide angle calculations

The figure below illustrates the slide plate, as it was first intended. The slide plate corresponds to the height of the sandfill holes used in the final design. The calculations of slide plate length and angle for SB and Olivin were made using the formulas given in section 3.2.2. The figures on the next page illustrate the results.

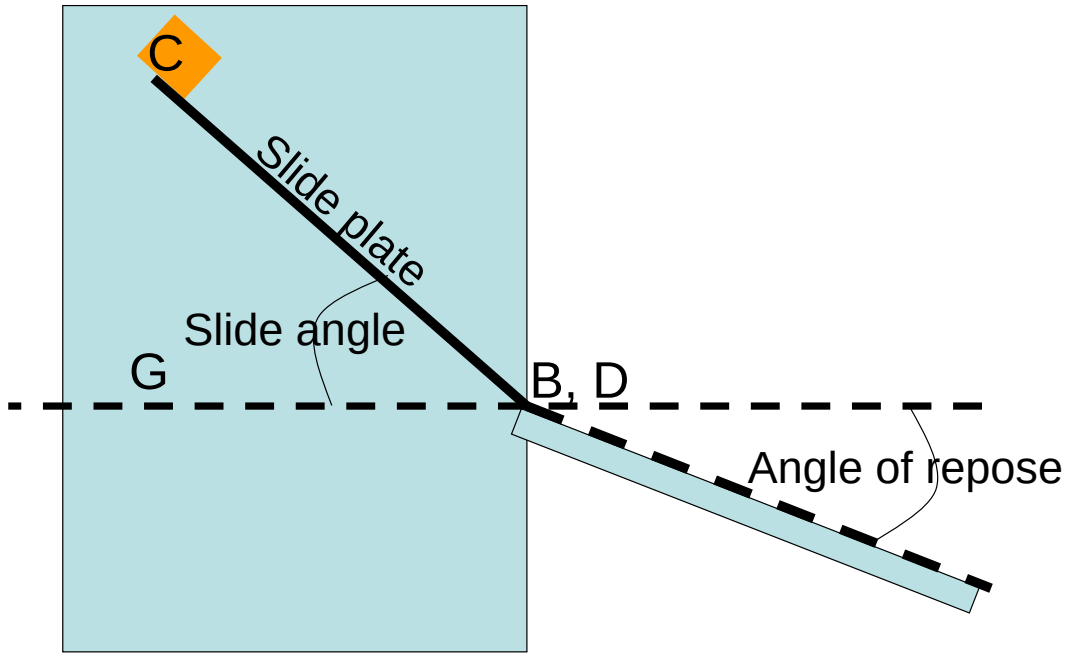

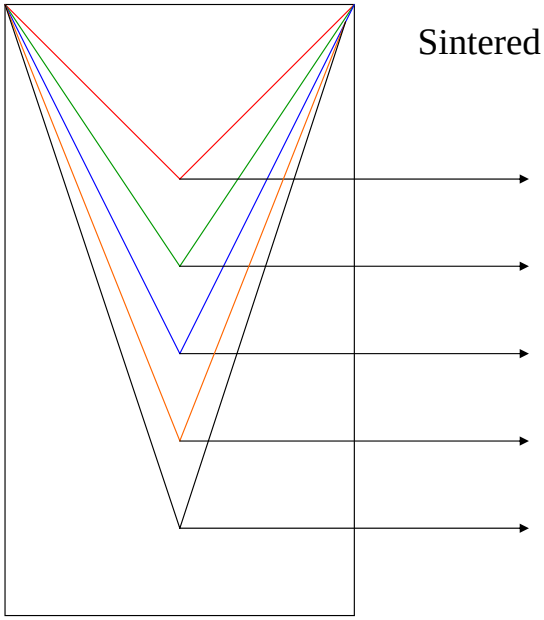

Sintered bauxite 20/40

Y=4 cm slide angle=31,5

Y=6 cm slide angle =26,4

Y=8 cm slide angle =24,4

Y=10 cm slide angle =23,5

Y=12 cm slide angle =22,9

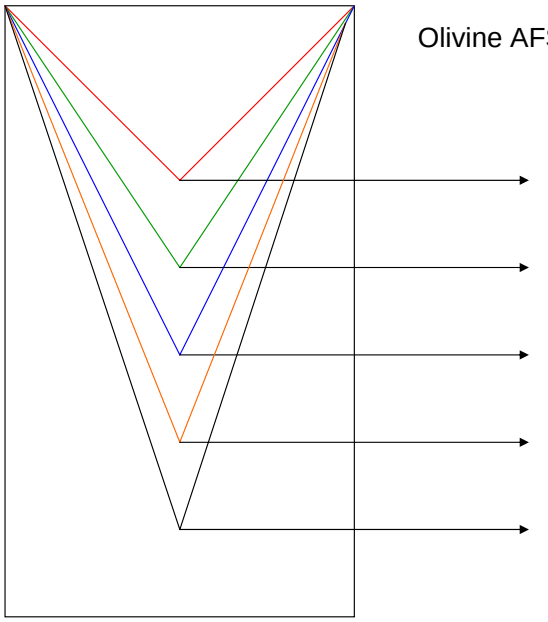

Olivine AFS30

Y=4 cm slide angle =43,6

Y=6 cm slide angle =35,9

Y=8 cm slide angle =33

Y=10 cm slide angle =31,7

Y=12 cm slide angle =30,9

Appendix C

Insulation and thermoelement characterization

Produktdatablad

Rockwool Lamellmatte 541

Rockwool Lamellmatte 541 er produsert av fukt- og vannavvisende lameller av steinull, pålimt en glassfiberarmert og PE-belagt alufolie. Steinullens fiberretning er vinkelrett på overflatens plan, og det oppnås derfor en relativt høy trykkstyrke kombinert med lav vekt. Benyttes til termisk-, kondens- og frostisolering av ventilasjonskanaler, rør, beholdere og tanker.

MONTERING
På ventilasjonskanaler, rør, mindre tanker og beholdere anbefales det at en lamell fjernes fra folien, slik at man i lengderetningen får en overlapp. Denne stiftes så med en spesial stiftemaskin før aluminiumstape klebes over alle skjøter, både tverrgående og langsgående. Ytterligere sikring kan også gjøres med ståltråd etter taping. På horisontale og rektangulære kanaler med bredde over 300 mm, anbefales det at mattene klebes eller festes mekanisk til kanalens underside. Samme utførelse kan også anbefales for sirkulære kanaler med stor diameter.

VARMELEDNINGSTALL

Middeltemp. °C	0	25	50	75	100
λ W/mk	0,039	0,041	0,046	0,053	0,062

Rockwool Lamellmatte 541 er tilsluttet TIK -kontrollen, Danmark.

BRANN
Ullen er ubrennbar i henhold til ISO 1182

FUKT
Ca. 0,004 vol.% ved 90% relativ fuktighet.

NOMINELL DENSITET
Ca. 35 kg/m³

TRYKKSTYRKE
Sammentrykning ved belastning 5 kN/m²: 10 mm (gjelder for tykkelse 50 mm).

MAKS ANVENDELSESTEMPERATUR
Ullside: 250°C
Overflatebelegg: 80°C

VANNABSORPSJON
<1 vol.% i henhold til BS 2972:75.

DIMENSJONER

Tykkelse (mm)	Bredde (mm)	Lengde (mm)	Innhold- m²/pk
25	1 000	10 000	10,0
30	1 000	8 000	8,0
40	1 000	5 000	5,0
50	1 000	5 000	5,0
60	1 000	4 000	5,0
80	1 000	2 500	2,5
100	1 000	2 500	2,5

EMBALLASJE
Lamellmatte 541 er pakket i plastsekker.

HELSE OG MILJØ
Produkter av isolasjonsull er ikke brennbare, de råtner ikke og de absorberer ikke fuktighet og lukt. De er ikke utsatt for angrep av meldugg, mugg eller bakterier. Isolasjonsmaterialene er fri for formaldehyd, og er blant de byggematerialer som har minst utstråling av radon, slik at enhver fare kan utelukkes. Det er dokumentert gjennom toksikologiske forsøk at Rockwool ikke avgir giftige gasser ved brann. Det er ikke sannsynlig at det kan utvikle seg allergier ved arbeid med isolasjonsull. Forskning og medisinske undersøkelser gjennom 50 år viser ingen økning i sykdommer hos mennesker som er eksponert for isolasjonsull. Verdens Helseorganisasjon, WHO, konkluderer med at produktene utgjør minimal eller ingen helserisiko.

KVALITETSSIKRING
Rockwool isolasjon produseres etter den strengeste kvalitetskontroll som tilfredsstiller kravene i den internasjonale kvalitetsstandard NS-EN ISO 9001.

På grunn av kontinuerlige prosessforbedringer forbeholder A/S Rockwool seg til enhver tid retten til å endre produktspesifikasjonene uten varsel.

A/S Rockwool, Nydalsveien 21 Telefon: 22 02 40 00 Kundeservice: 22 02 40 50
Postboks 4215 Nydalen, 0401 Oslo Telefaks: 22 15 91 78 E-mail kundeservice: ordre@rockwool.no

ROCKWOOL® BRANNSIKKER ISOLASJON

Thermal Ceramics

Superwool™ 607™ HT VF Products

Product Information

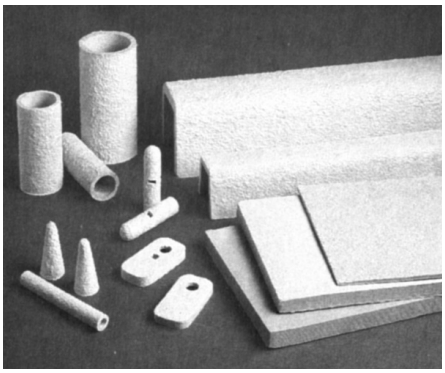

DESCRIPTION

Superwool™ 607™ HT VF Products is a vacuum formed insulating product, made from a mixture of Superwool™ 607™ HT fibres, refractory constituents and organic binders.

Vacuum-forming allows the production of a variety of configurations, tailored to the particular application and ranging from simple sections (such as tubes, cones and flat shapes) to complex shapes (such as combustion chambers).

Good cohesive strength, high operating temperature and excellent insulating properties make Superwool™ 607™ HT VF Products suitable to various applications.

TYPE

Vacuum formed shapes manufactured from high temperature insulation wool.

CLASSIFICATION TEMPERATURE

1300°C (ENV 1094-3)

The maximum continuous use temperature depends on the application. In case of doubt, refer to your local Thermal Ceramics distributor for advice.

STANDARD GRADES

VF 607HT
Standard formula based on Superwool 607HT fibre.

VF 607HT D
Dense formula based on Superwool 607HT fibre.
High resistance against molten iron and steel.

FEATURES

- Easy to use
- 'Tailor made' shapes
- Homogeneous structure
- Low thermal conductivity
- Good erosion resistance and rigidity
- Excellent hardness properties
- Excellent thermal shock resistance
- Low heat storage, lightweight
- Good cycling performance (standard formula)
- Molten iron & steel resistance
- No reaction with alumina based bricks in application in the range of typical use temperature
- Flame resistant
- Easy to machine
- Exonerated from any carcinogenic classification under nota Q of directive 97/69 EC

THE QUEEN'S AWARDS FOR ENTERPRISE 2003

Termoelement med kabel

Type TK

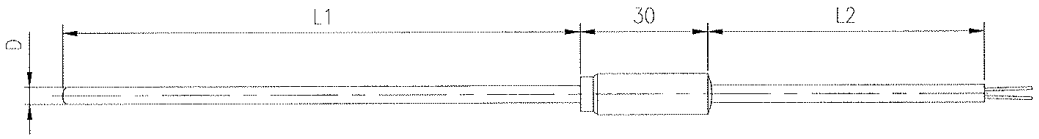

Tegn.nr. H32138

Bestillingskode

Føler diameter - D

1,0 mm
1,5 mm
3,0 mm
6,0 mm
8,0 mm

Målepunkt

R - Isolert
G - Jordet
E - Eksponert

Element

1 - Enkelt element
2 - Dobbelt element (tilgjengelig mantel, se tabell side 220)

Mantel materiale

B - Inconel
C - 316 SS
D - 310 SS
N - Nicrobell-C
V - Hastelloy-X

Kalibrering

K - NiCr-Ni
J - Fe-CuNi
T - Cu-CuNi
N - NiCrSi-NiSi

Føler lengde - L1

L1 - Spesifiseres (mm)

Kabel type

P - PVC -30/ +80°C
S - Silikon -50/ +180°C
T - Teflon -70/ +250°C

Kabel lengde - L2

L2 - Spesifiseres (mm)

Kontakt

U - Uten kontakt
SM - Standard HAN
SF - Standard HUN
MM - Mini HAN
MF - Mini HUN

Lagerførte varianter, se side: 230
Lagerført mantel, se side: 220
Komp.fitting på forespørsel, se side: 700

TK - 3,0 - R - 1 - B - K - L1 - T - L2 - U

Teck Instrument AS
Tlf: (+47) 32 24 13 00 *Fax:* (+47) 32 24 13 01
E-post: salg@teck.no *Internett:* www.teck.no